Multiscale Imaging of Concrete

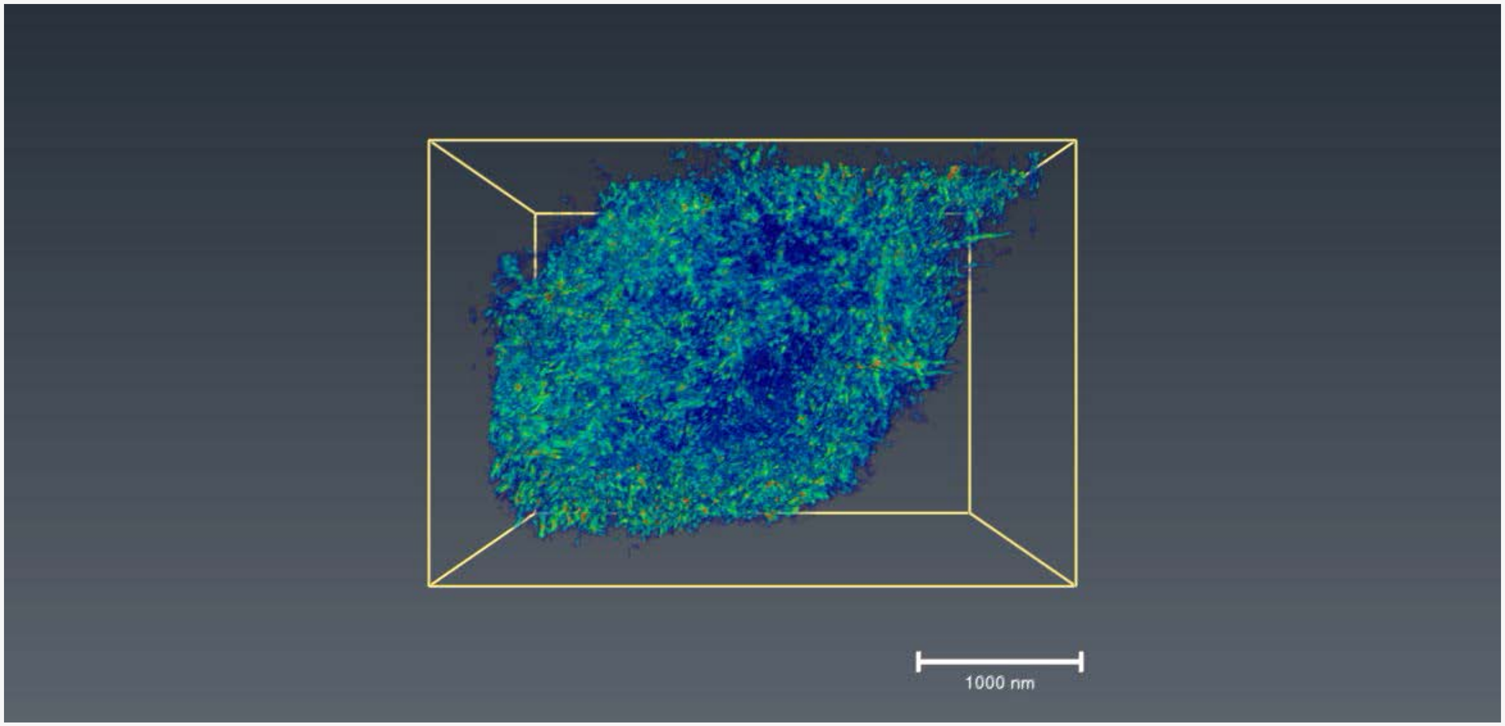

Paulo Monteiro
Department of Civil and Environmental Engineering
University of California at Berkeley

Need for multiscale imaging

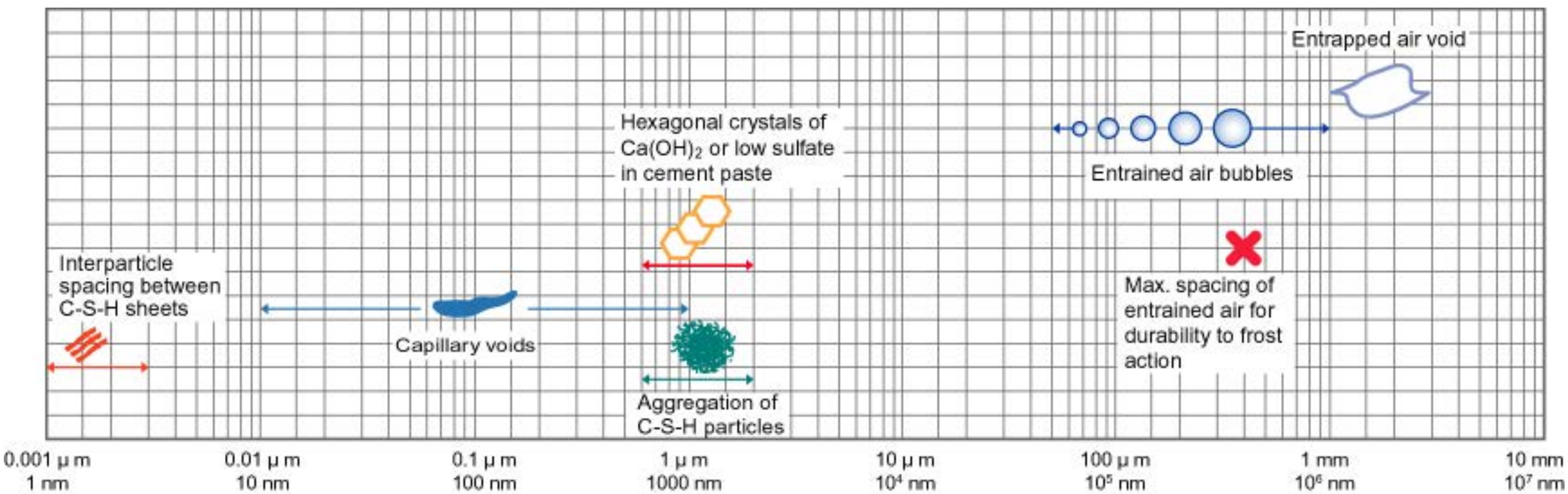

The New York Times

N.Y. / REGION

With Connecticut Foundations Crumbling, 'Your Home Is Now Worthless'

By KRISTIN HUSSEY and LISA W. FODERARO JUNE 7, 2016

http://www.nytimes.com/2016/06/08/nyregion/with-connecticut-foundations-crumbling-your-home-is-now-worthless.html?_r=0

Combining techniques at the micro/nano scale

Micro-tomography

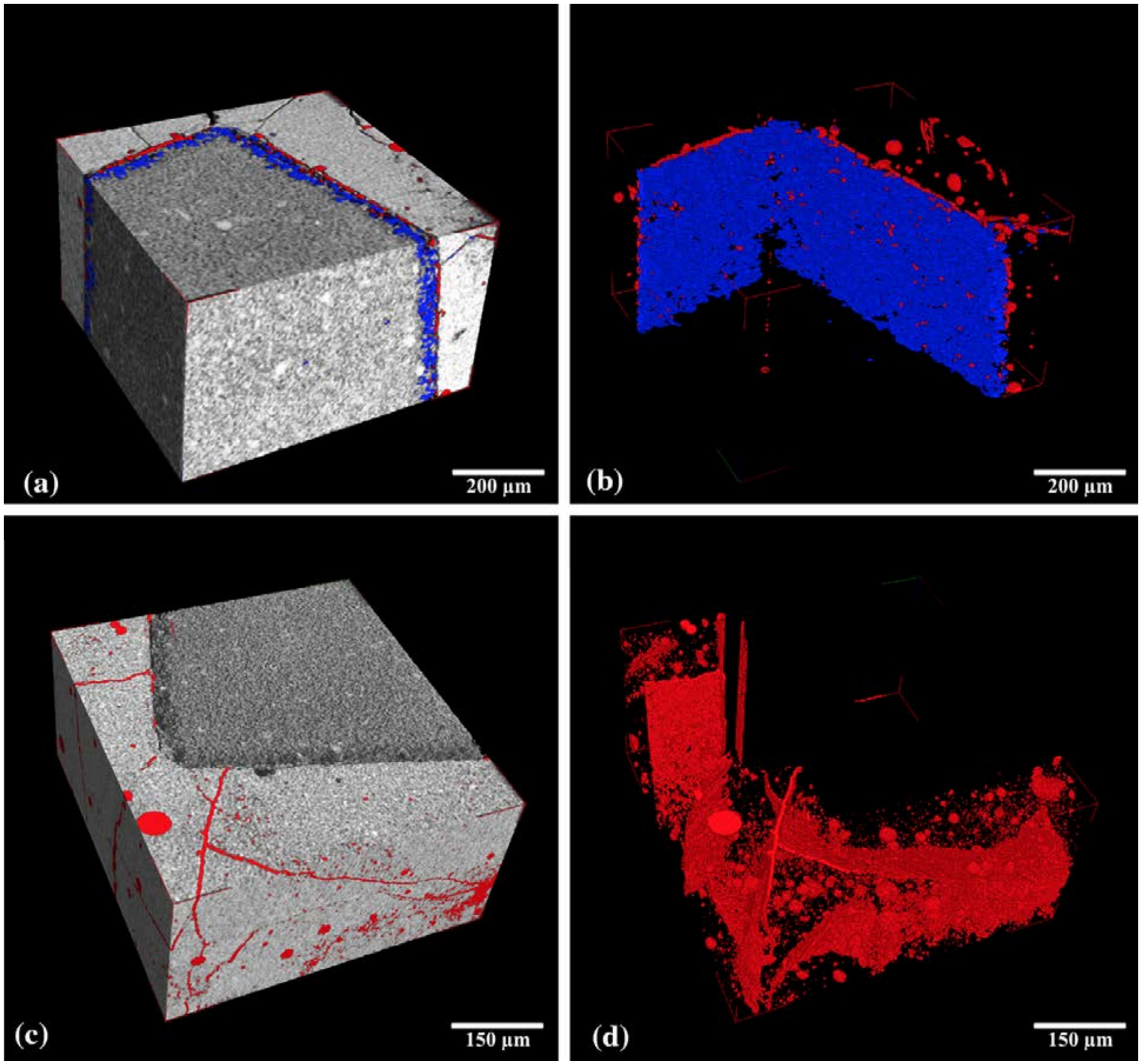

Marinoni et al., 2015

a) subvolume rendering showing dissolution zone in chert (blue) and debonding (red);
c) rendering of the subvolume with microcracks (red) emanating from the aggregate particle

MicroCT: SYRMEP beamline (ELETTRA)

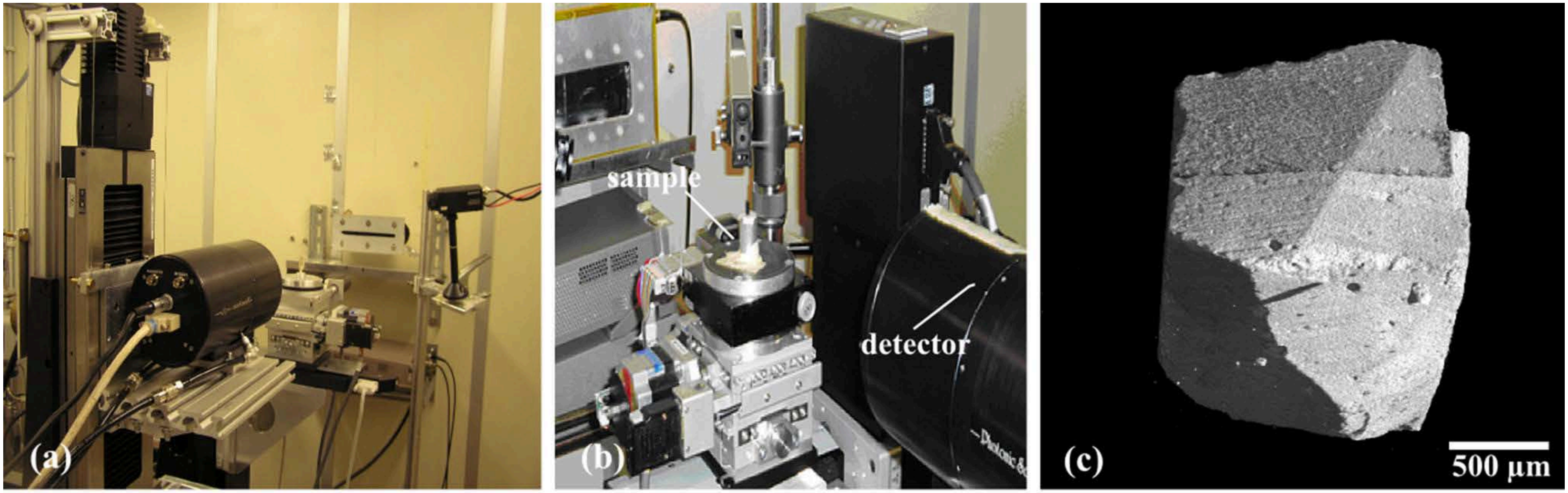

MicroXRD: SYRMEP beamline (ELETTRA)

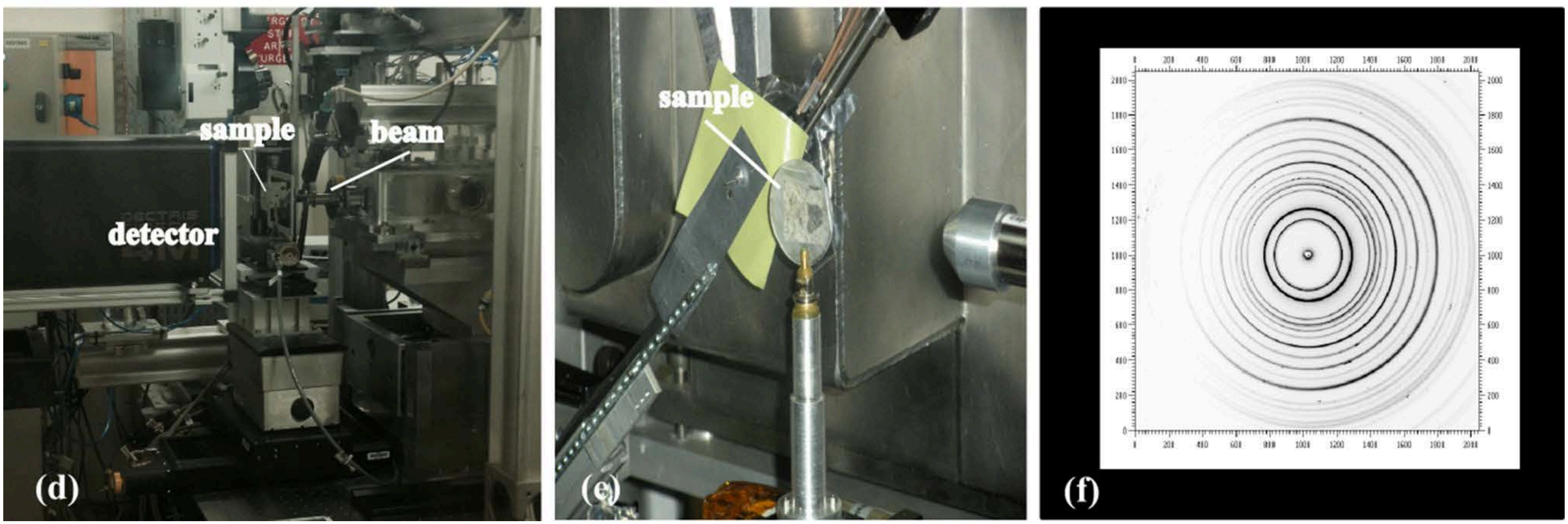

Mineralogy can be studied with microXRD

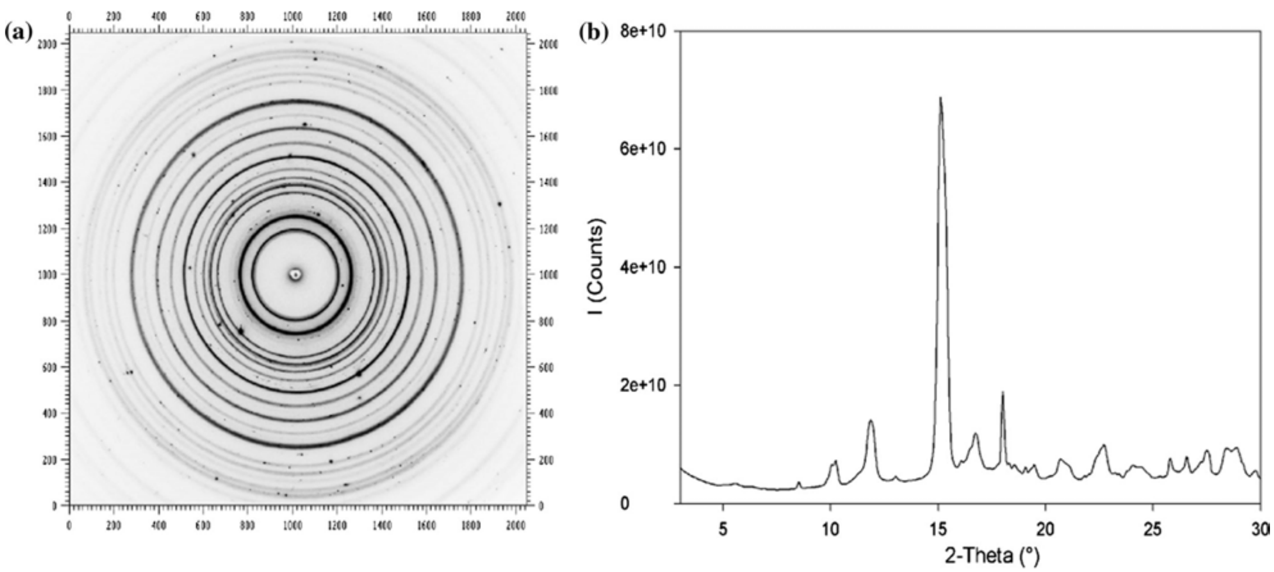

Chert near the interface.

Mean peaks → quartz

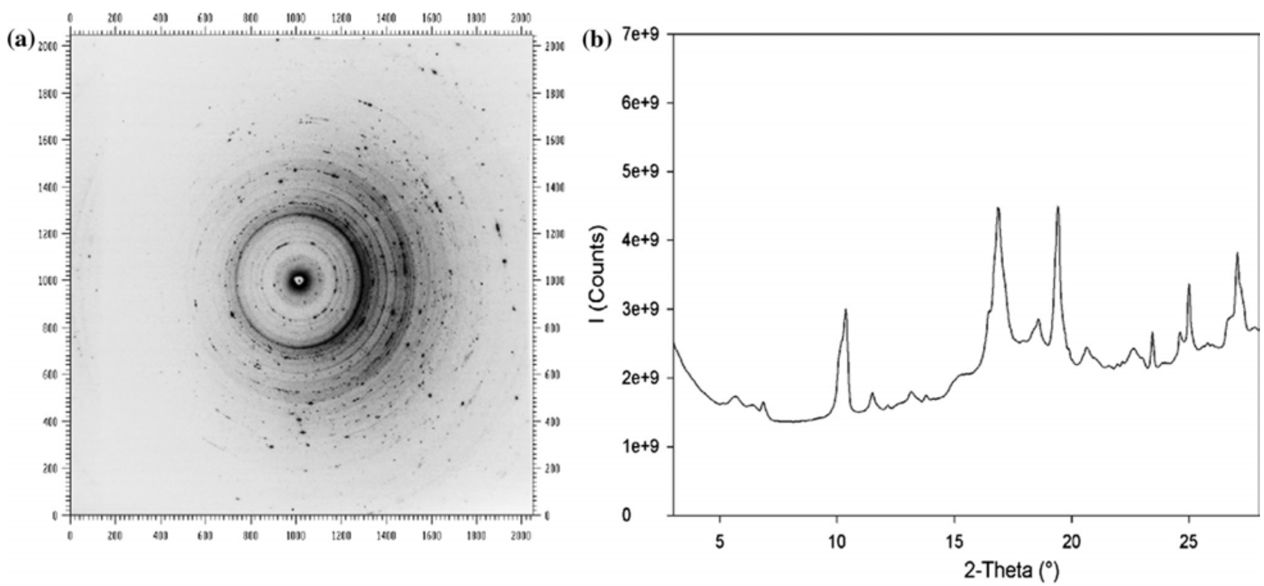

Chert near the interface.

Mean peaks → calcite

Quartz has dissolved away

Poro-mechanical model with chemical and mechanical damage

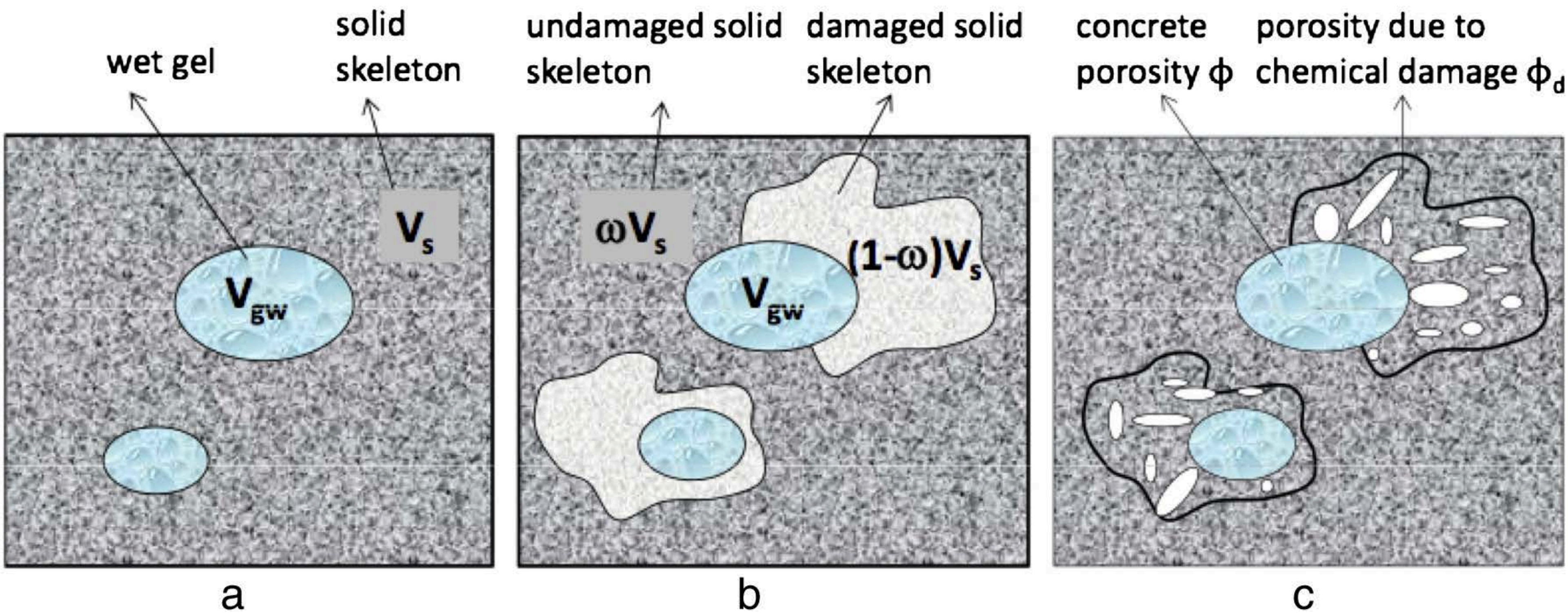

R. Pignatelli et al. / Cement and Concrete Research 53 (2013) 196–210

$$(1-d)=\frac{(1-D_{ch})\left[(1-\omega)K_s+Mb^2\right]-Mb^2}{(1-\omega)K_s}$$

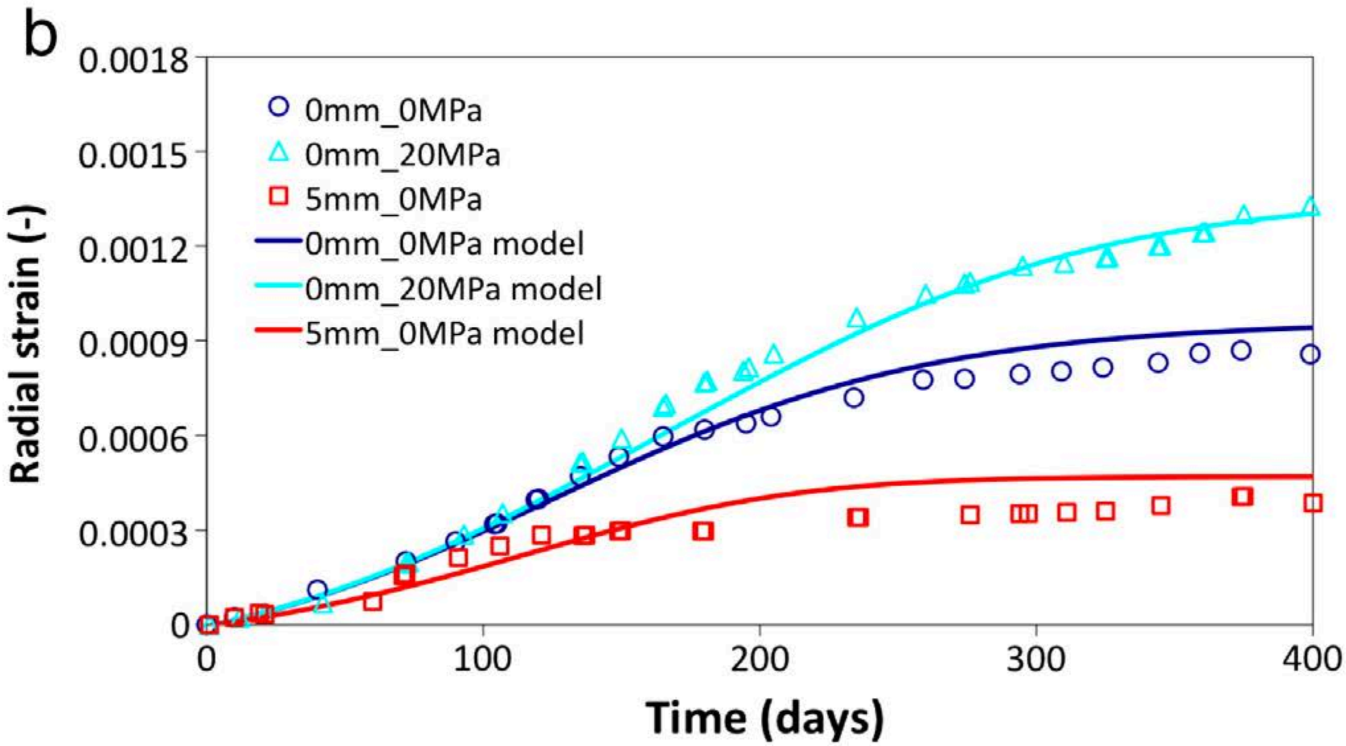

Studies of shales at the nanoscale

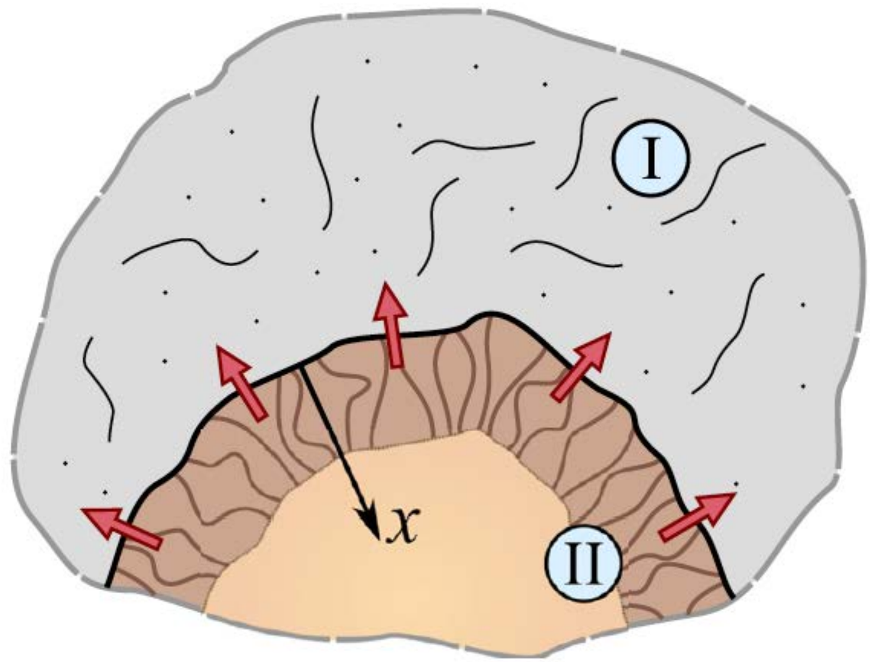

(I) a porous, fissurized matrix and
(II) a kerogen inclusion with very low permeability

P.J.M. Monteiro et al, *PNAS*, Vol 109, No.50, 20309–20313, 2012

A mathematical model of fluid and gas flow in nanoporous media

Paulo J. M. Monteiro[a,b], Chris H. Rycroft[c,d], and Grigory Isaakovich Barenblatt[c,d,e,1]

$$\partial_t p = \chi \partial_x (\partial_x p)^{m+1}, \quad \chi = \frac{A\rho_0}{\alpha\mu\phi}$$

for the case of weakly compressible fluid and

$$\partial_t p = \kappa \partial_x \left(p (\partial_x p)^{m+1} \right), \quad \kappa = \frac{A}{\mu\phi}$$

production rate per unit of area

$$\begin{aligned} Q &= Sj_n \\ &= S\rho_0 u_n = \frac{S\rho_0}{\mu}\left(\frac{df(0)}{d\xi}\right)^{m+1} \frac{P^{m+1}}{[\chi(t-t_0)P^m]^{(m+1)/(m+2)}} \\ &= \frac{SA\rho_0}{\mu} P^{\frac{2(m+1)}{m+2}} [\chi(t-t_0)]^{-\frac{m+1}{m+2}} \left(\frac{df(0)}{d\xi}\right)^{m+1}. \end{aligned}$$

- Finally, the production rate is given by:

$$Q = \frac{SA\rho_0}{\mu} P^{\frac{m+1}{m+2}} [\kappa(t-t_0)]^{-\frac{m+1}{m+2}} \left(\frac{df(0)}{d\xi}\right)^{m+1}. \qquad Q \sim (t-t_0)^{-(m+1)/(m+2)}$$

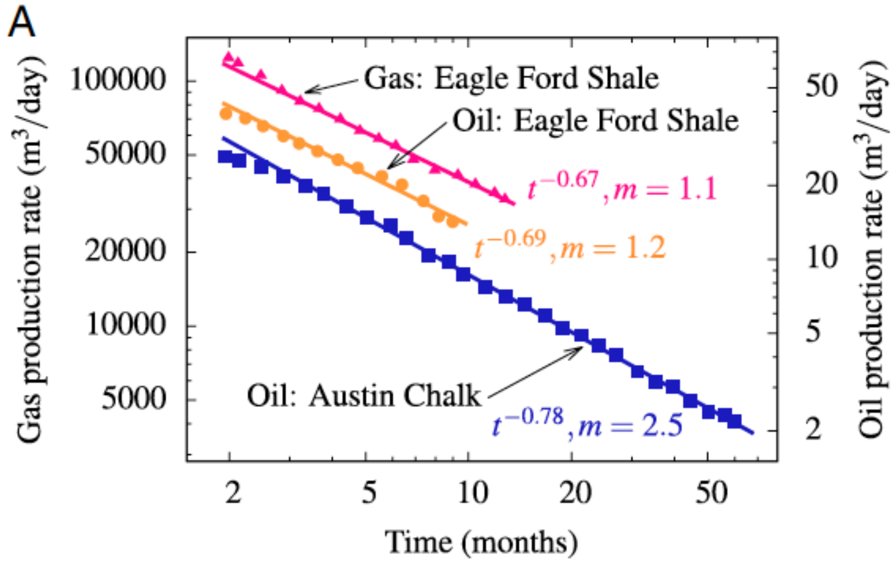

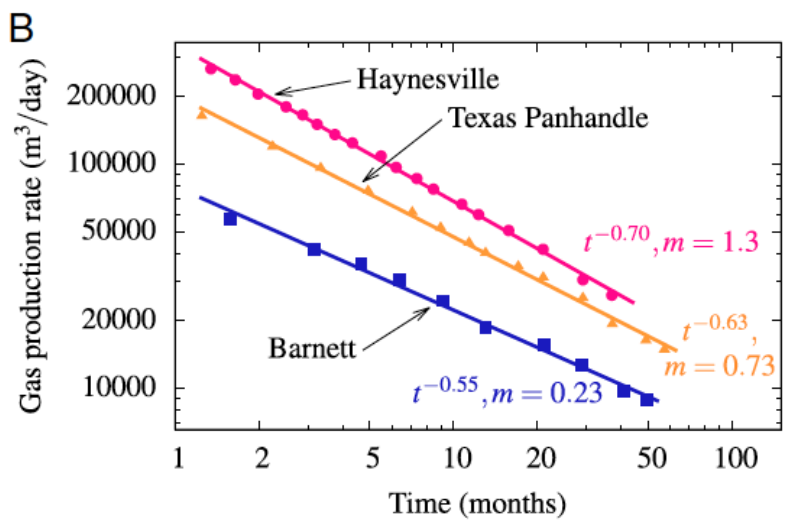

Nanoprobe at APS

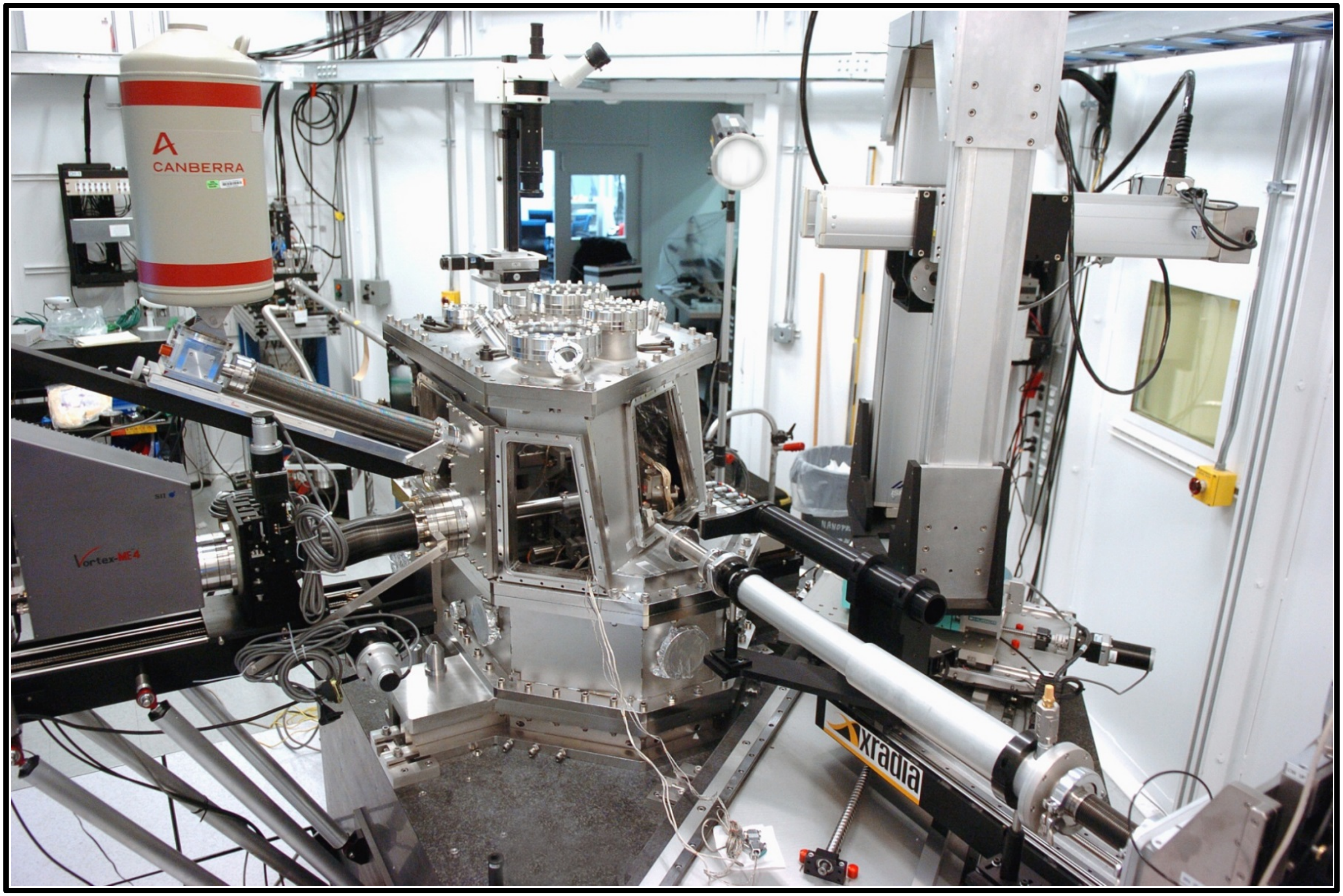

Preliminary tests for shale

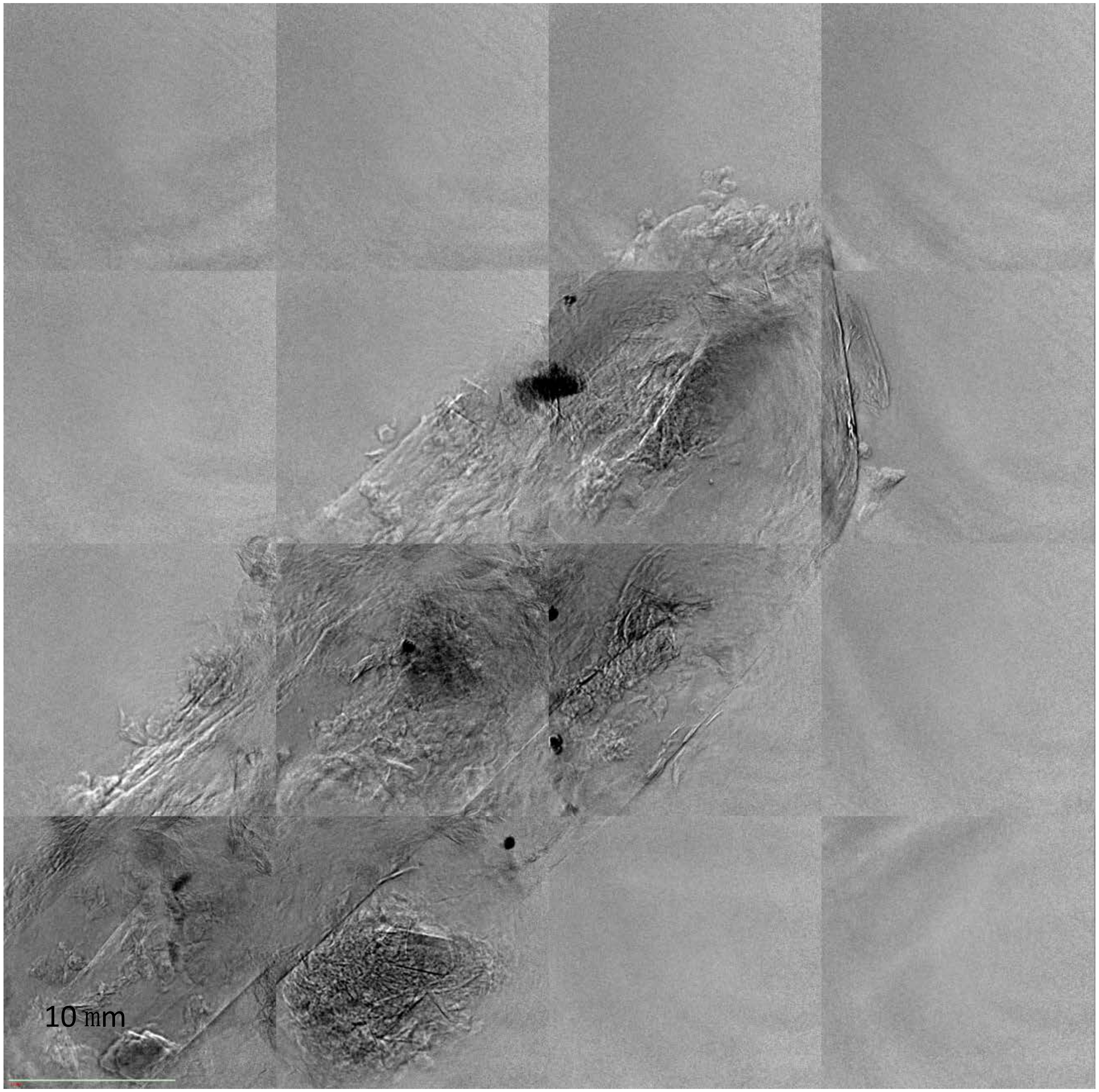

Imaging of shale using hard x-ray at APS. The images were stitched together to have a broad field of view of the particle. The pixel size was 16 nm with a spatial resolution of 30 nm.

Distribution of kerogen in a shale

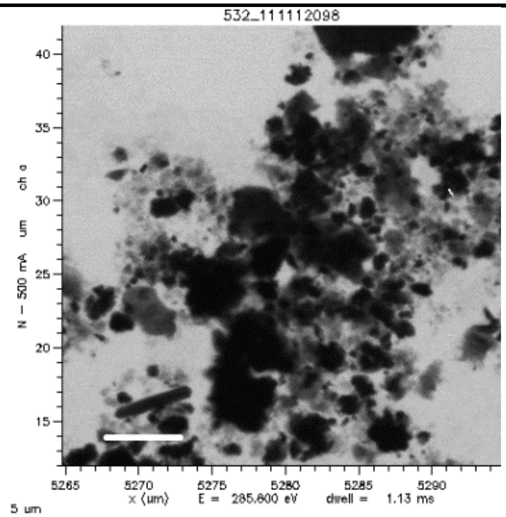

a)

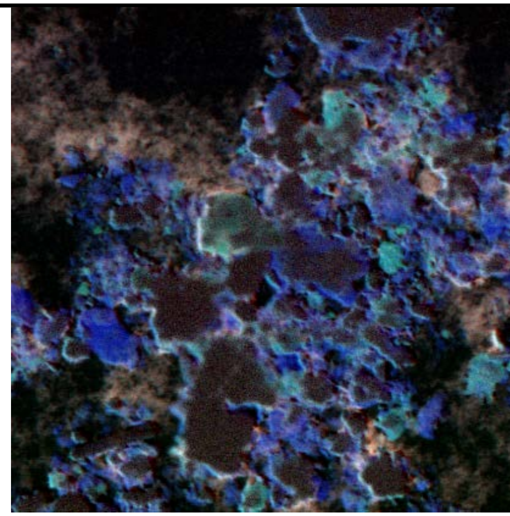

b)

Determination of the connectivity of organic matter in shales a) absorption image of shale. At this energy it is not possible to identify the various phases in shale; b) Synchrotron radiation allows for the fine-tuning of photon energy so it is possible to create high-resolution mapping of the location of the kerogen. Red: "Kerosene" peak at 286.7, Green: 296eV, Blue: "Shale" peak at 297eV.

Importance of the mesoscale

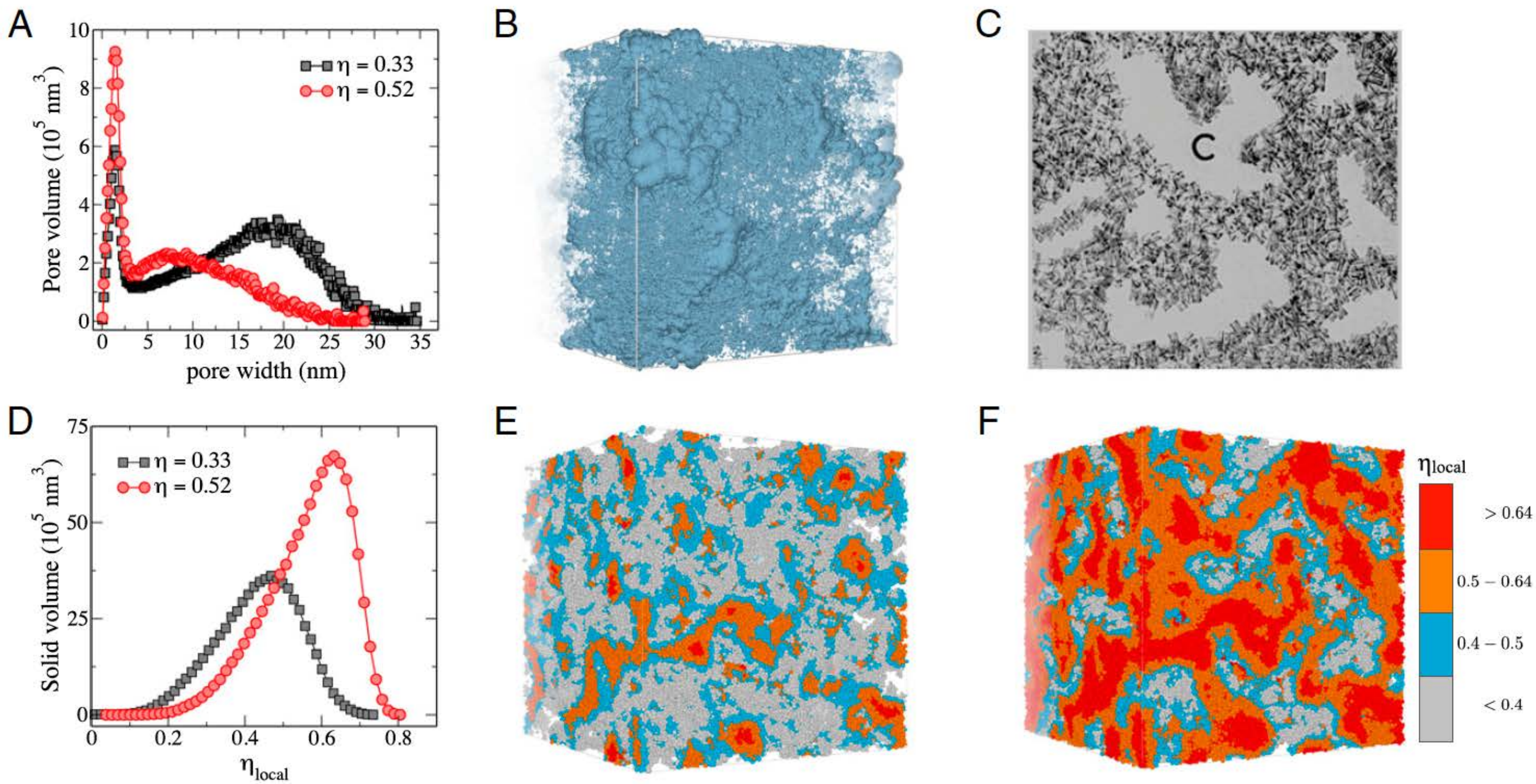

Fig. 1. (*A*) PSDs for $\eta = 0.33$ and $\eta = 0.52$. (*B*) Close-up view of the pore network for a sample with porosity $\phi = 0.48$, where $\phi = 1 - \eta$. The box size is $L = 195.22$ nm. (*C*) 2D schematic view of C–S–H. Reprinted from ref. 23. (*D*) Local volume fraction distributions η_{local} for $\eta = 0.33$ and $\eta = 0.52$. (*E*) Snapshot of a sample with $\eta = 0.33$ and (*F*) snapshot of a sample with $\eta = 0.52$ (the colors indicate η_{local} and $L = 585.54$ nm).

Ioannidoua et al., PNAS 2016

Nanoscale Characterization

- Spectromicroscopy

- Very high spatial resolution nanoCT

Scanning Transmission X-ray microscopy (STXM)

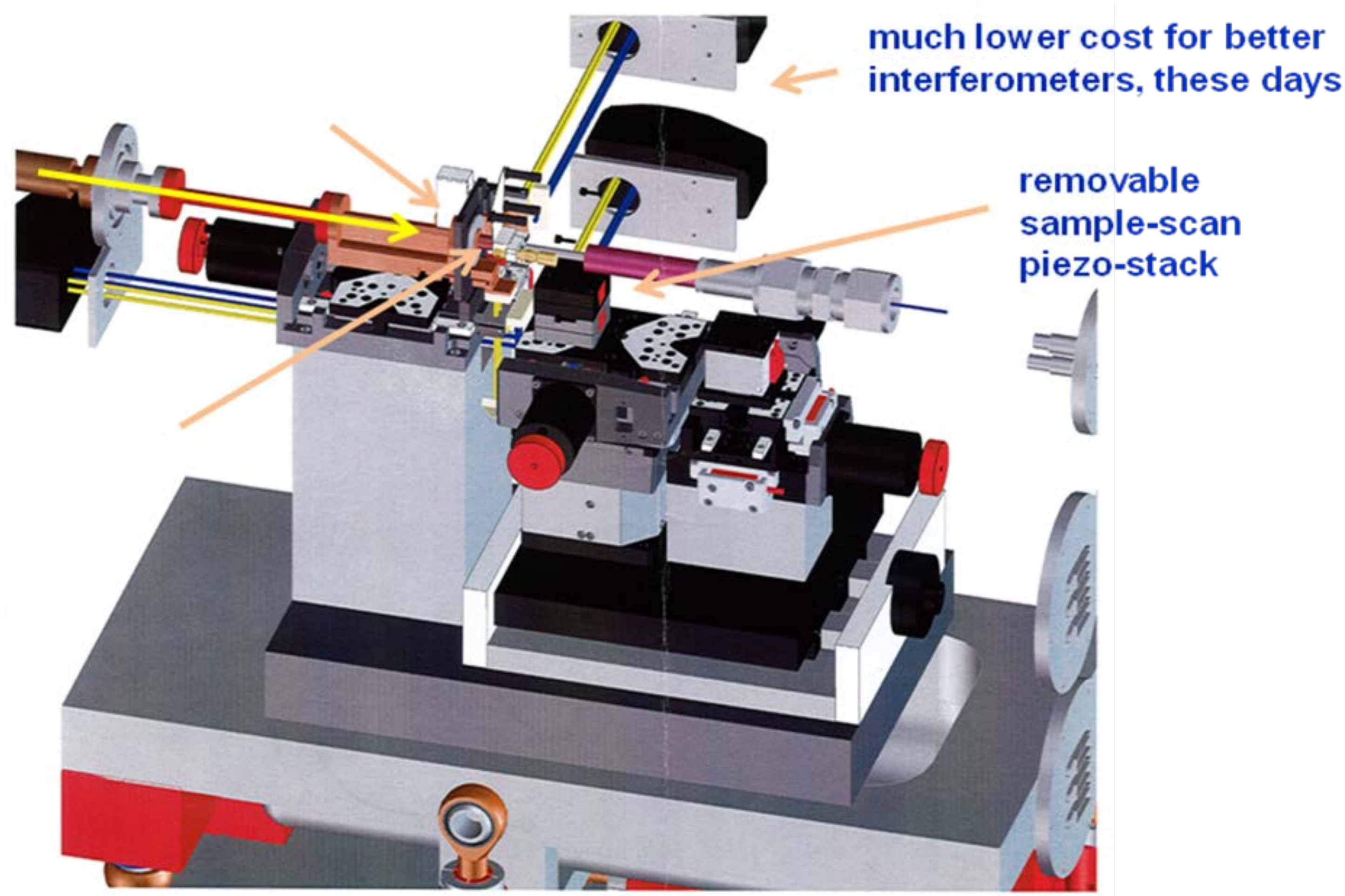

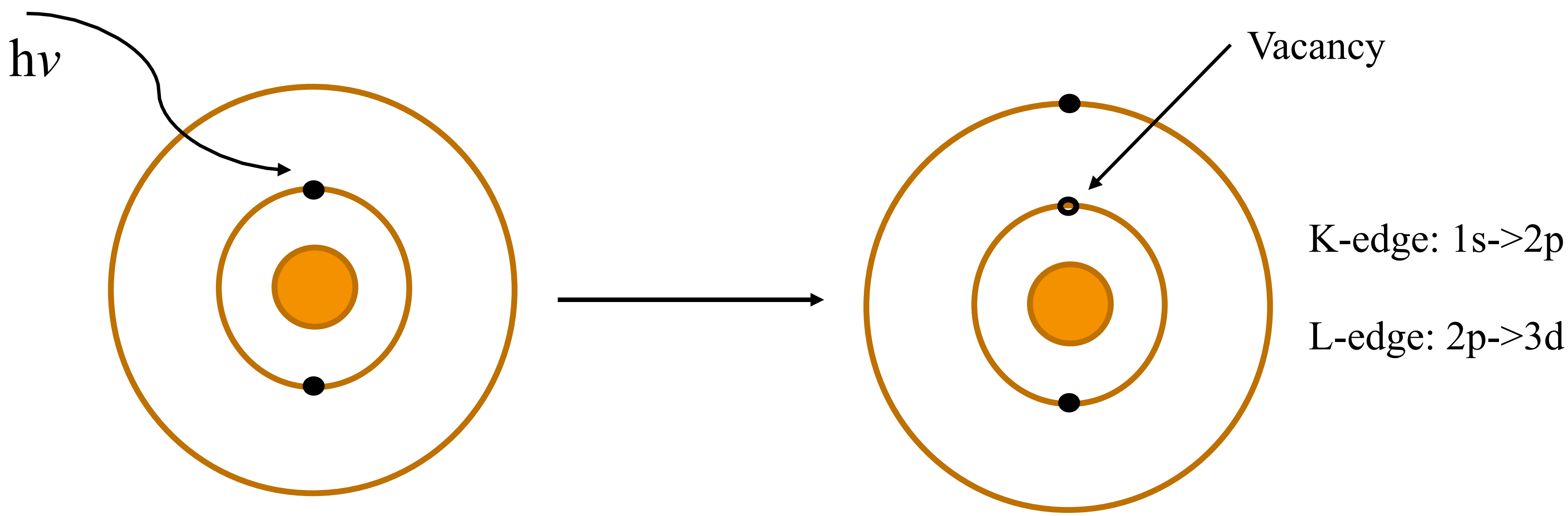
hν
Vacancy
K-edge: 1s->2p
L-edge: 2p->3d

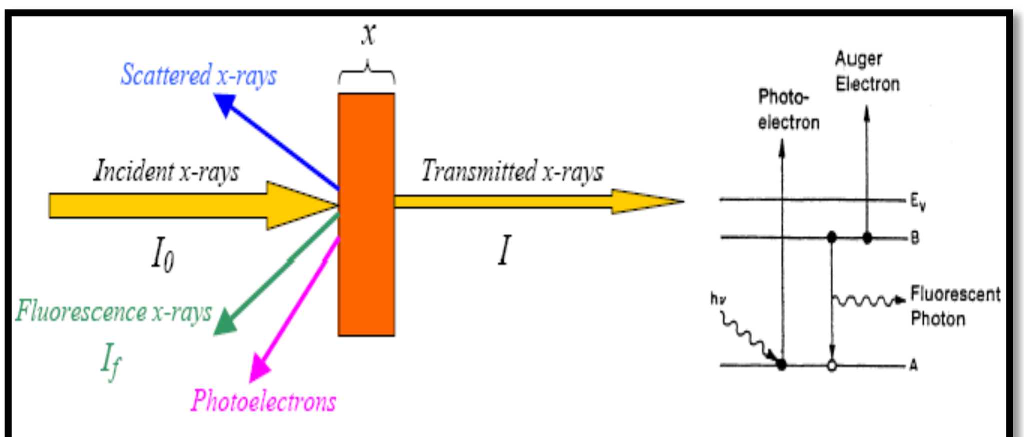
x
Scattered x-rays
Incident x-rays
Transmitted x-rays
I0
I
Fluorescence x-rays
If
Photoelectrons
Auger Electron
Photo-electron
Ev
B
hν
Fluorescent Photon
A

Absorption Edges

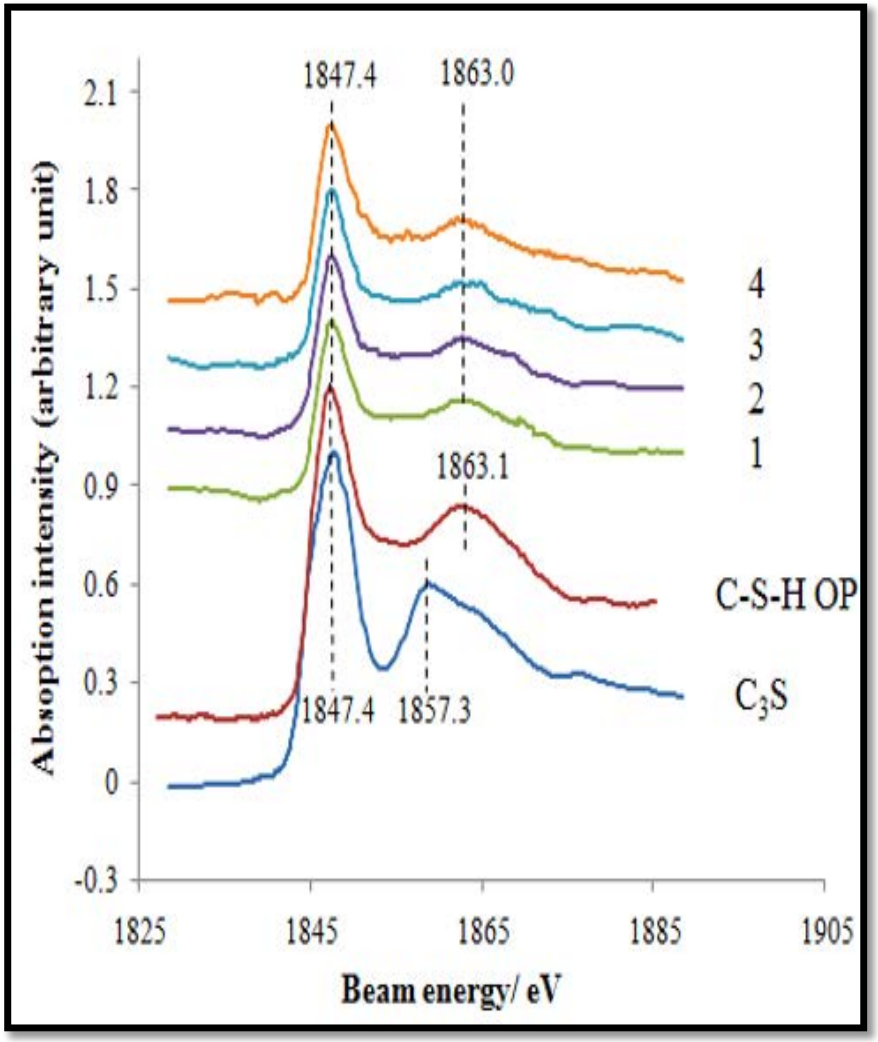

Cement Chemistry at Nanoscale

SCANNING MODE

- Image Scan
- Element Mapping
- Line Scan
- Stack Scan

Image Scan

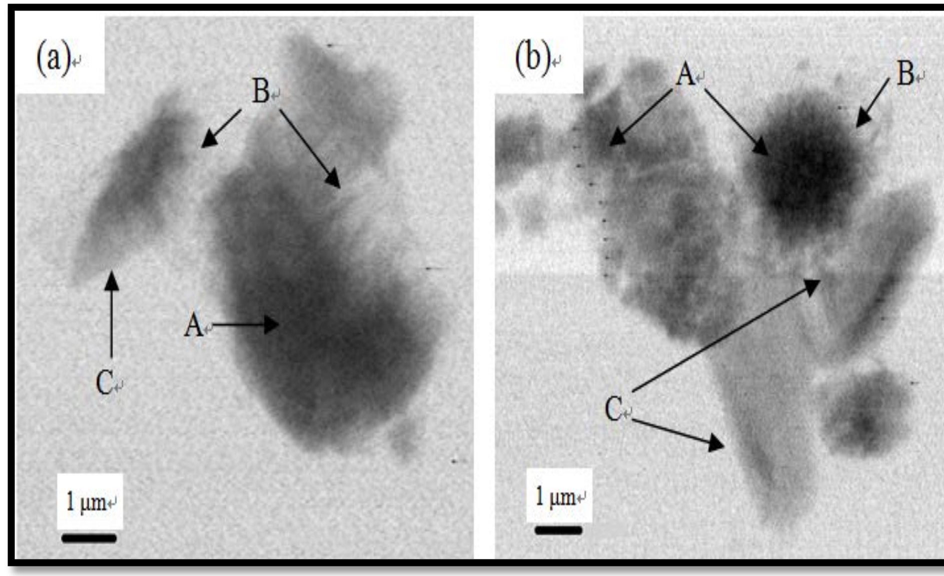

Element Mapping

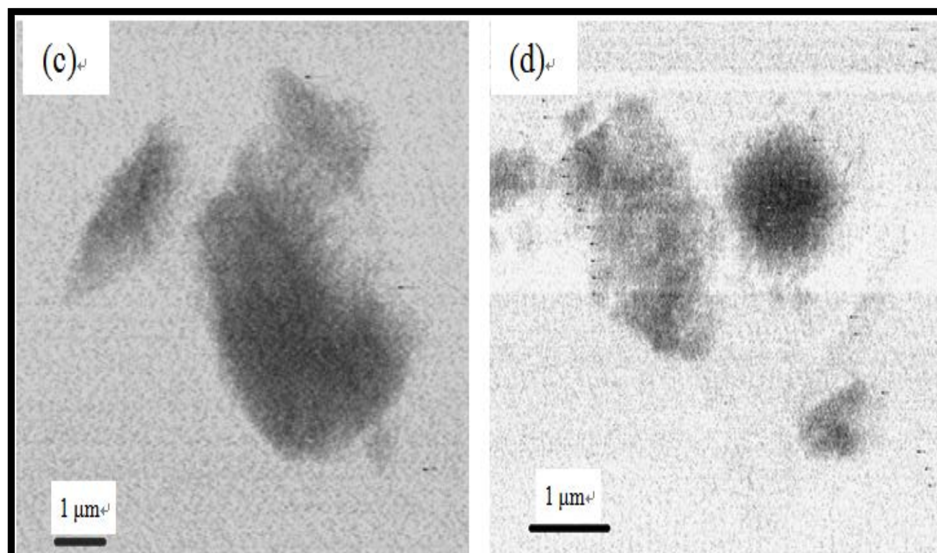

Line Scan

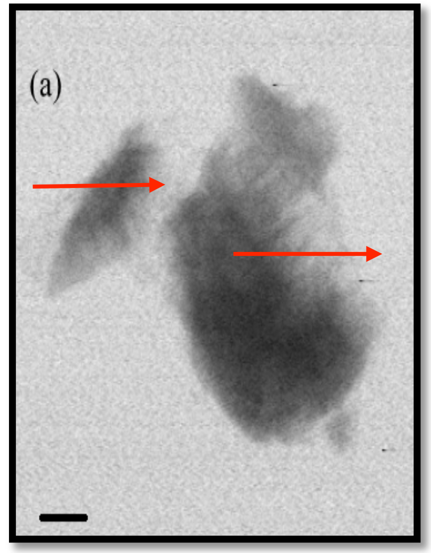

Stack Scan

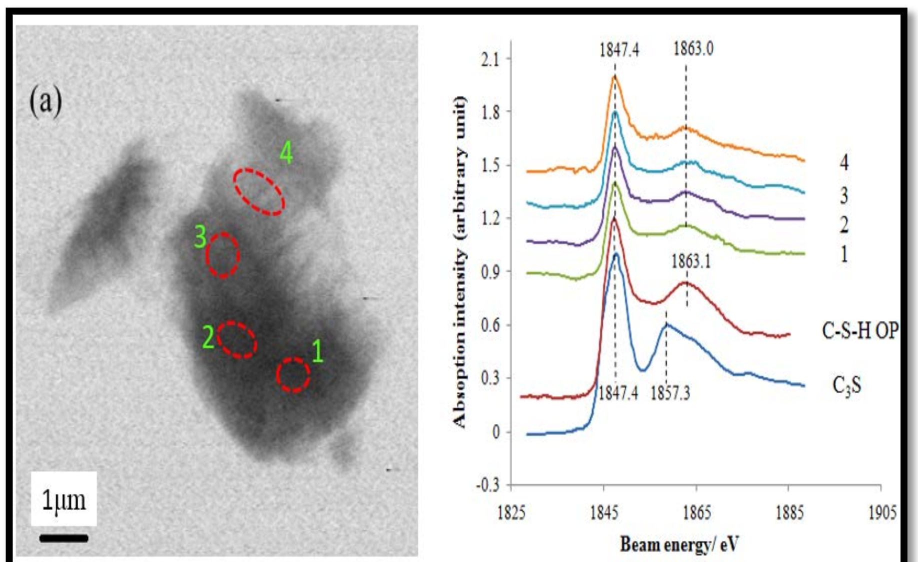

Study of the Ca-edge

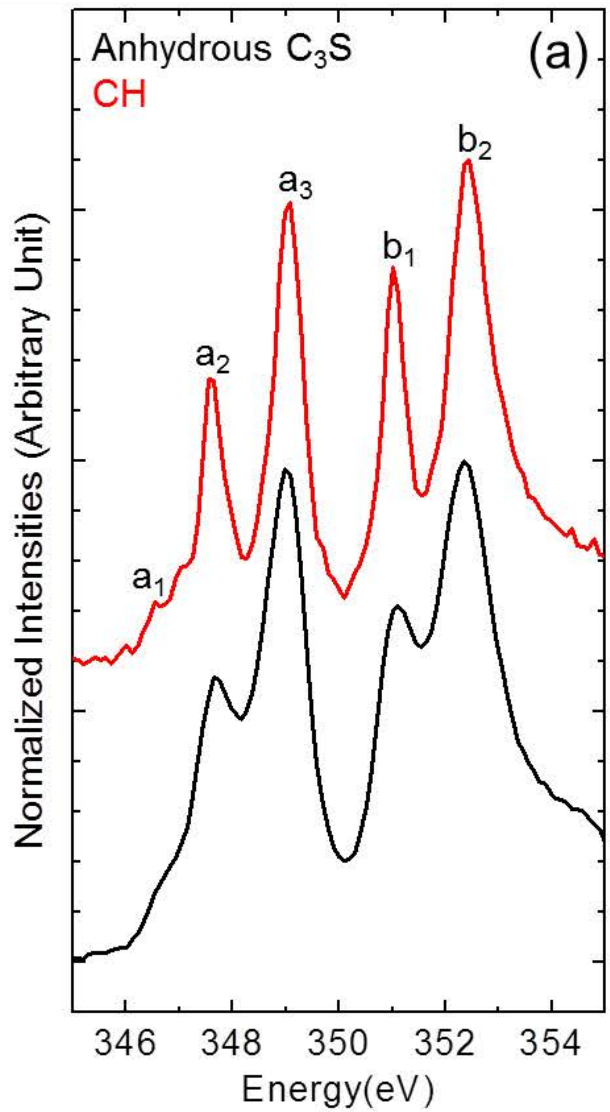

Study of the Ca-edge

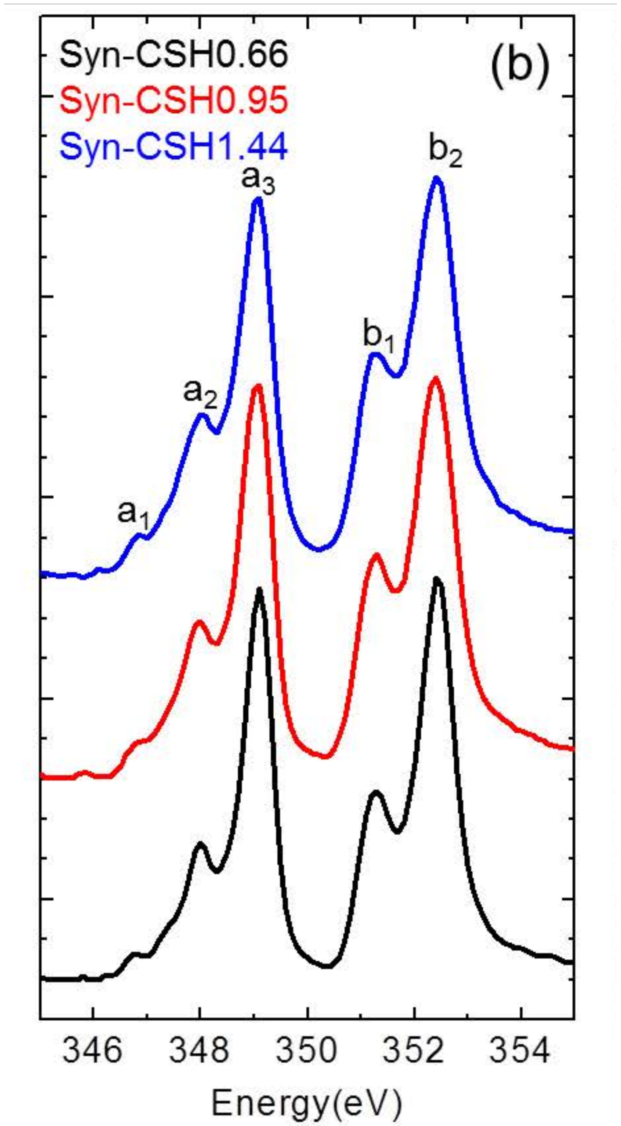

Study of the Ca-edge

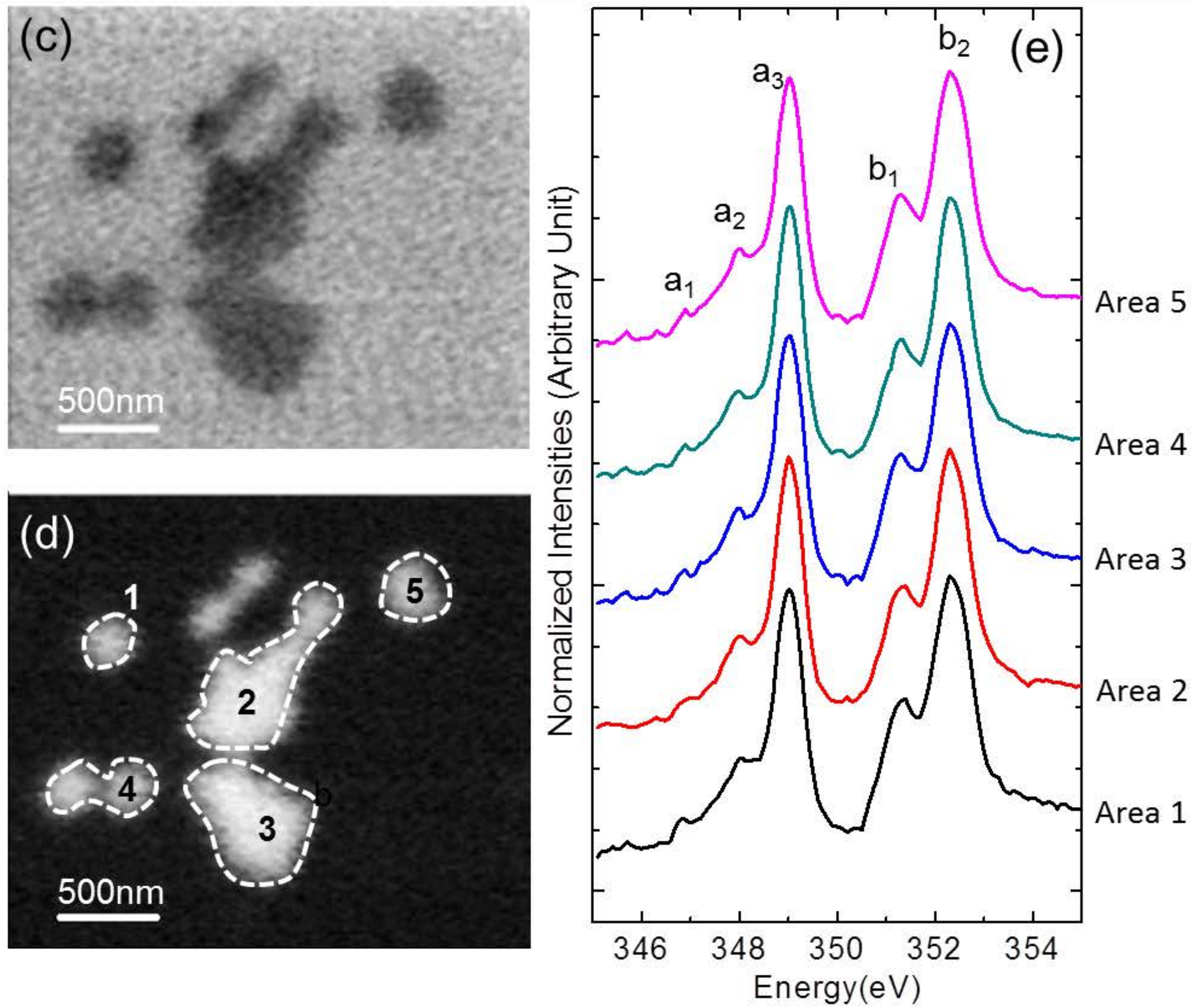

Study of the Si-edge for reference materials

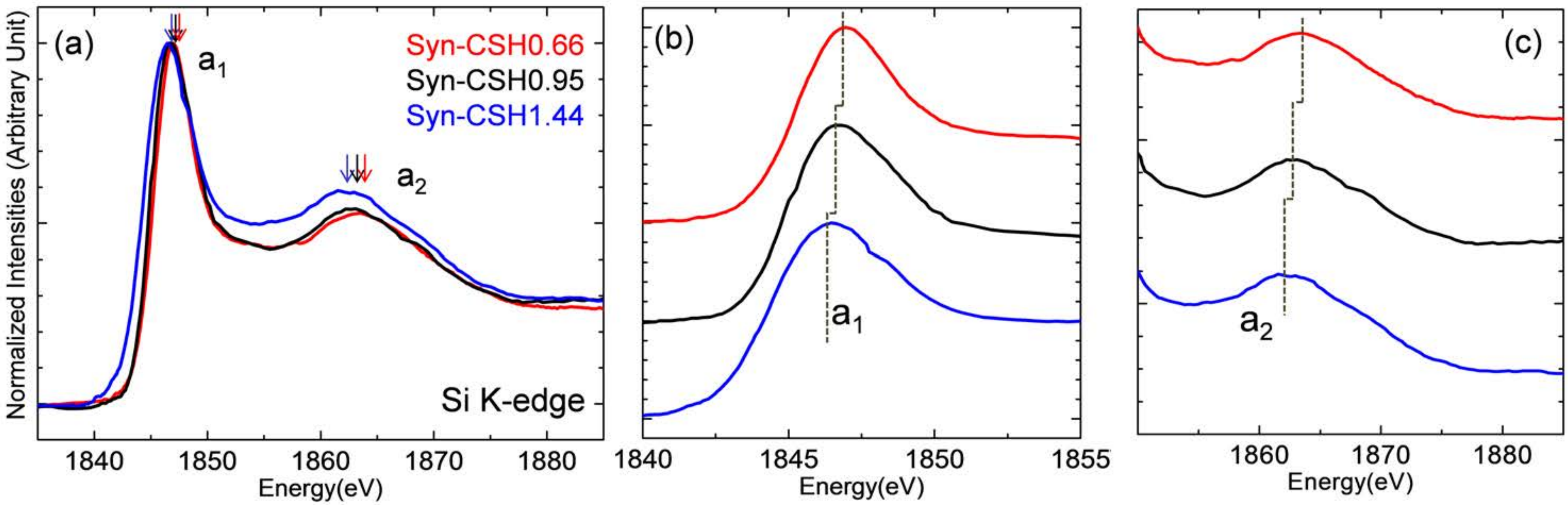

Hydrated C_3S (17day old sample)

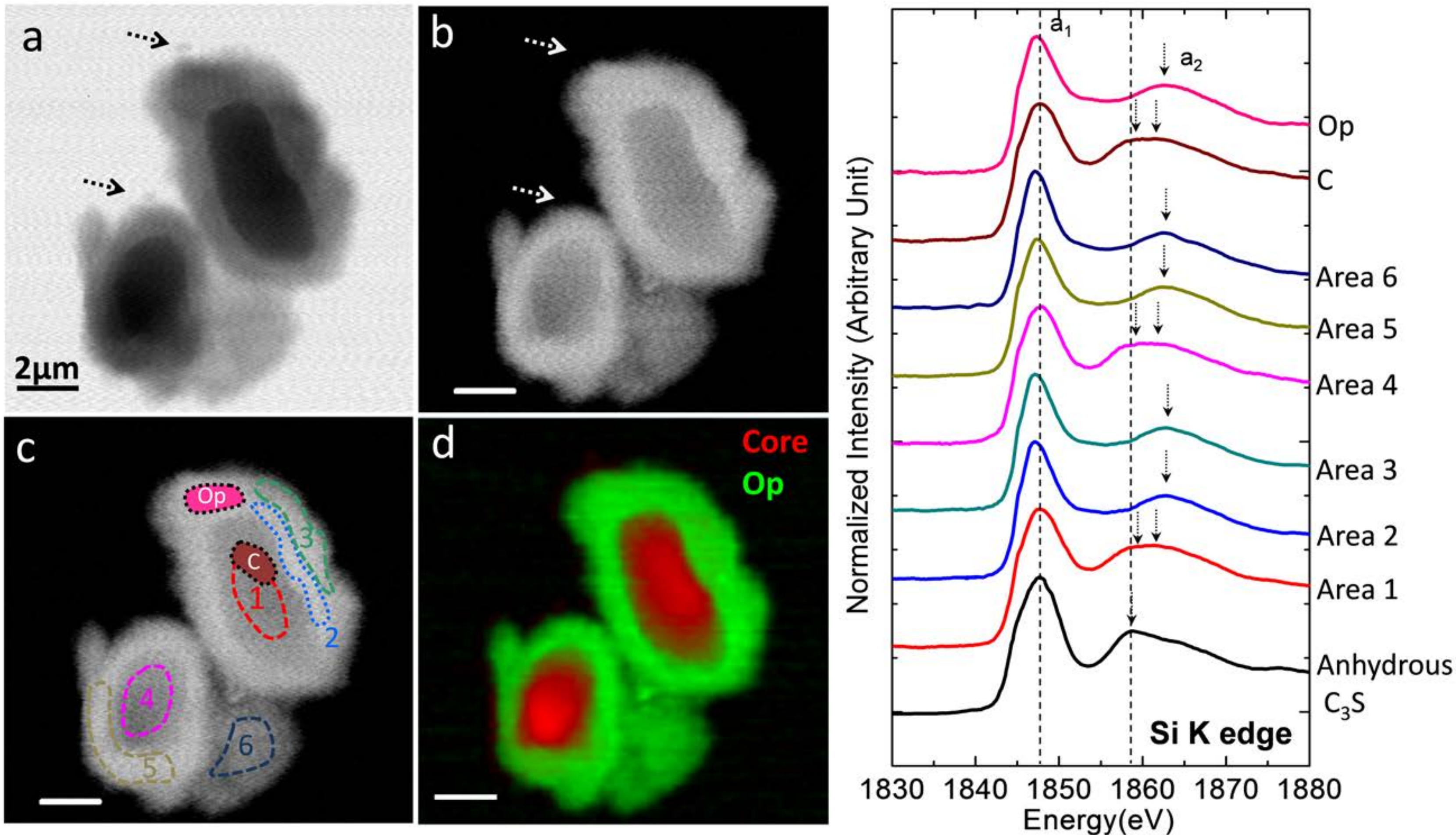

Older C_3S samples

1.5 years

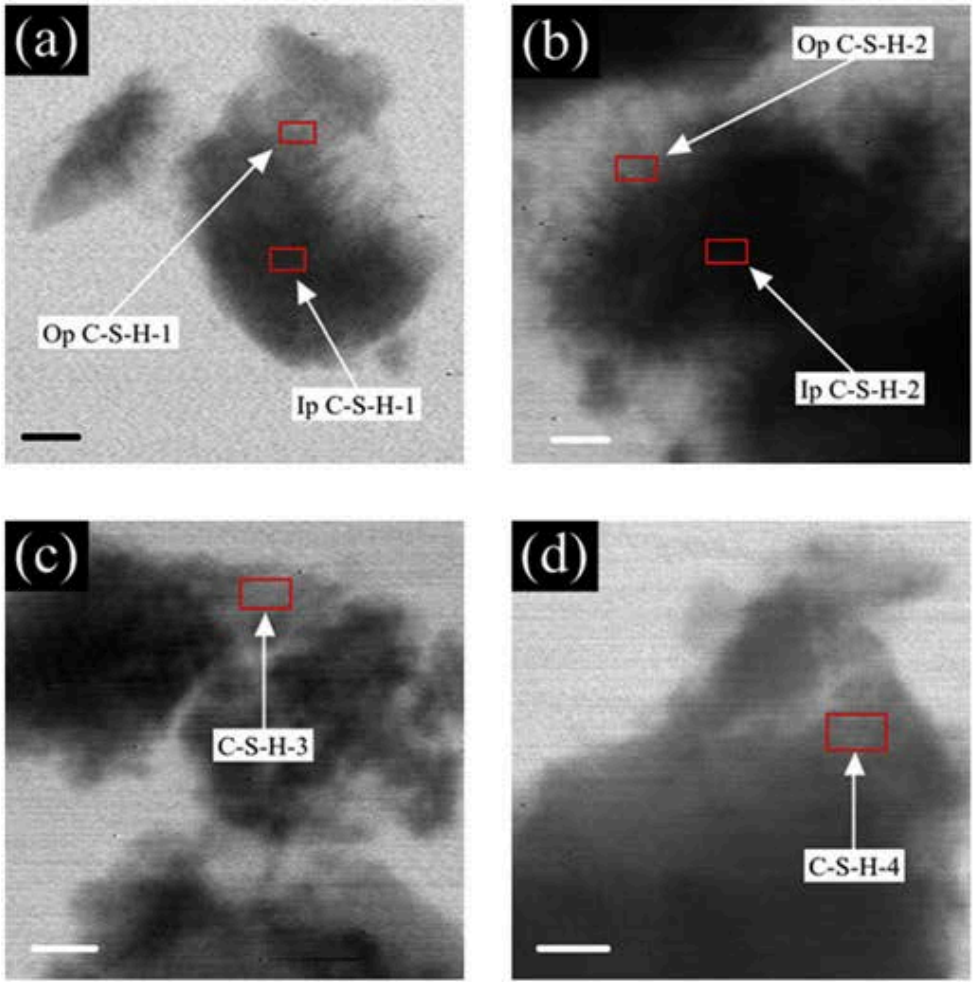

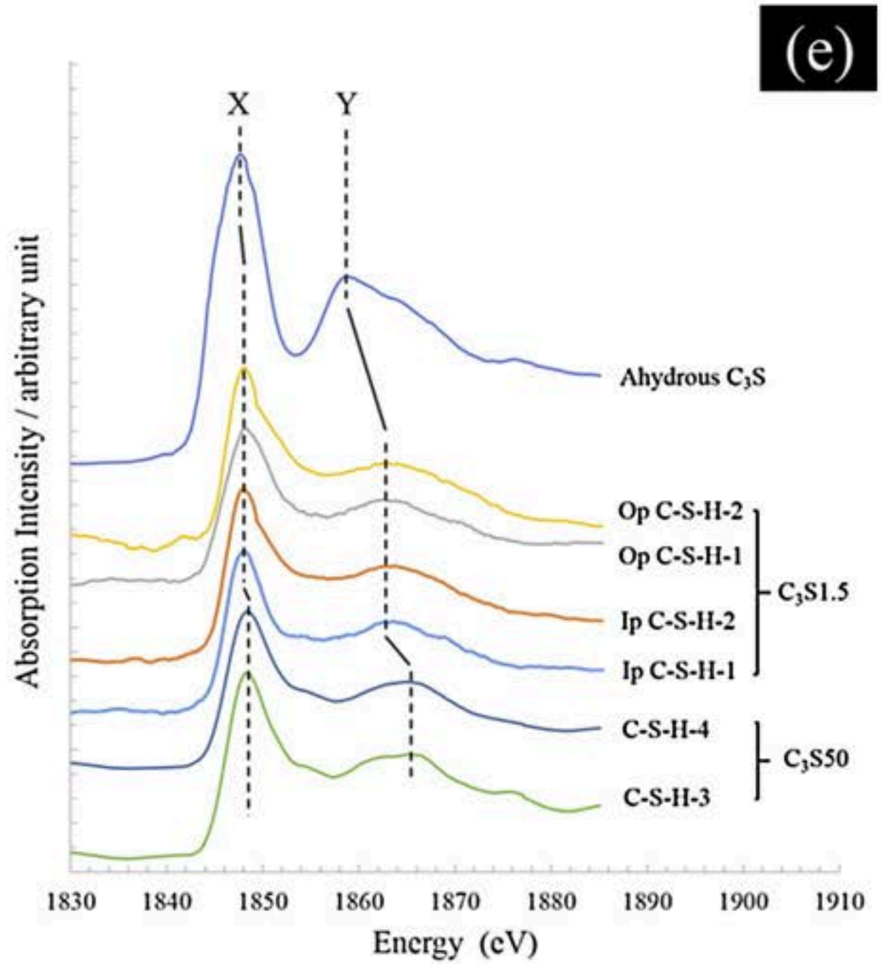

50 years

Geng et al., CCR, 2015

Energy difference, ΔE, between minor and major peak at Si K-edge.

	Sample	X (eV)	Y (eV)	ΔE (eV)	Hydration time (years)
	C_3S	1847.7	1858.9	11.2	0
	Ip C–S–H-1	1848.1	1860.9	12.8	1.5
$C_3S1.5$	Ip C–S–H-2	1848.1	1860.9	12.8	1.5
	Op C–S–H-1	1848.1	1861.1	13.0	1.5
	Op C–S–H-2	1848.1	1861.1	13.0	1.5
C_3S50	C–S–H-3	1848.3	1864.8	16.5	50
	C–S–H-4	1848.3	1864.8	16.5	50

Quantity of Si anions in each environment as a percentage obtained from integration of the peak areas.
Data from 12 h to 26 years are from Rodger [9].

Age	Q^0	Q^1	Q^2	MCL
12 h	89	11.0	0.0	2.00
1 day	68	30.0	2.0	2.13
7 days	48	43.0	9.0	2.42
14 days	33	52.0	15.0	2.58
1 month	30	53.0	17.0	2.64
3 months	18	62.0	20.0	2.65
6 months	14	65.0	21.0	2.65
1 year	10	55.0	35.0	3.27
2 years	6	52.0	42.0	3.62
26 years	0	42.0	58.0	4.76
50 years	0	47.9	52.1	4.18

Interactions between bi-polymer fiber/matrix

D. Hernández-Cruz et al. / Cement & Concrete Composites 48 (2014) 9–18

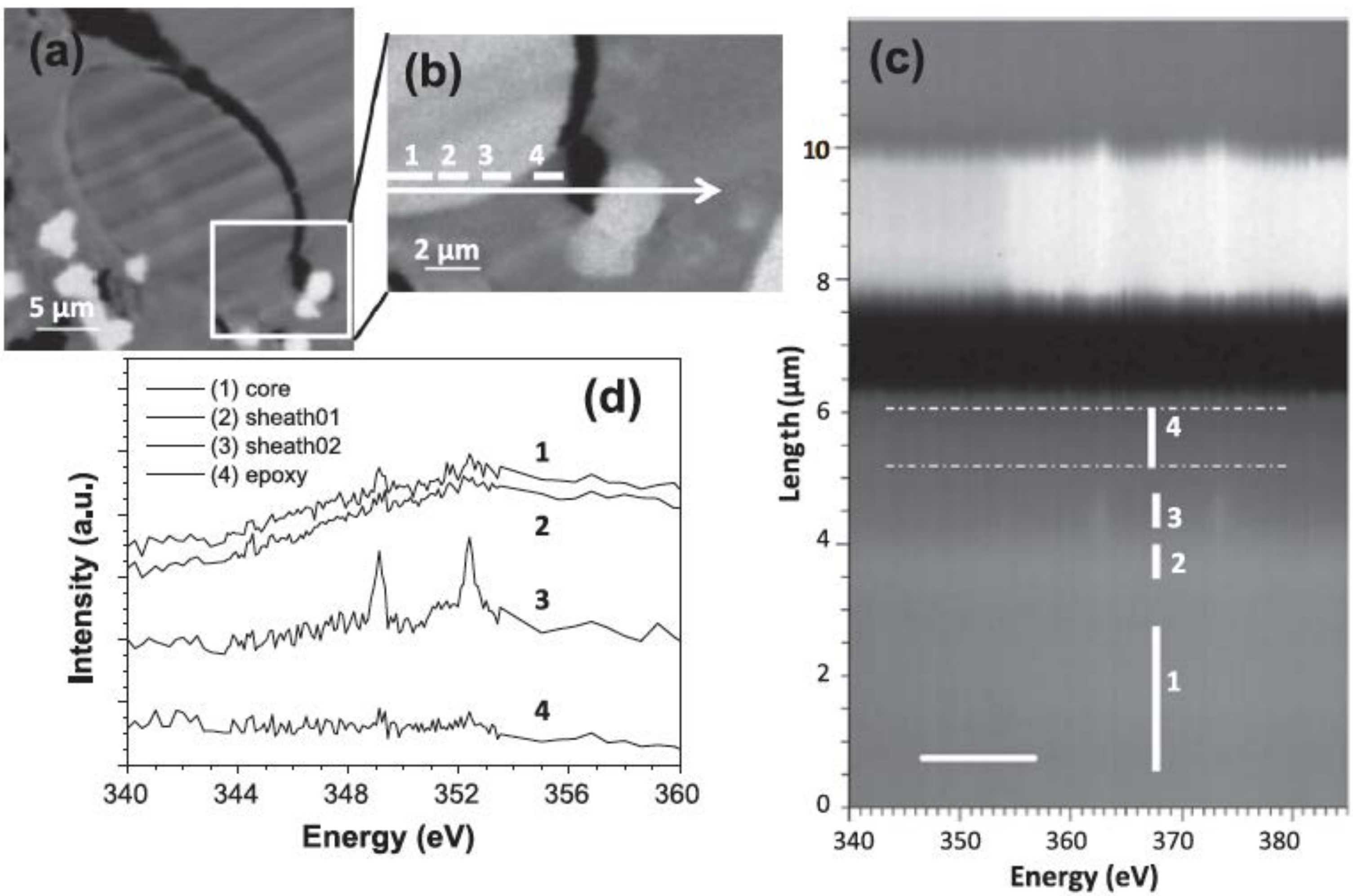

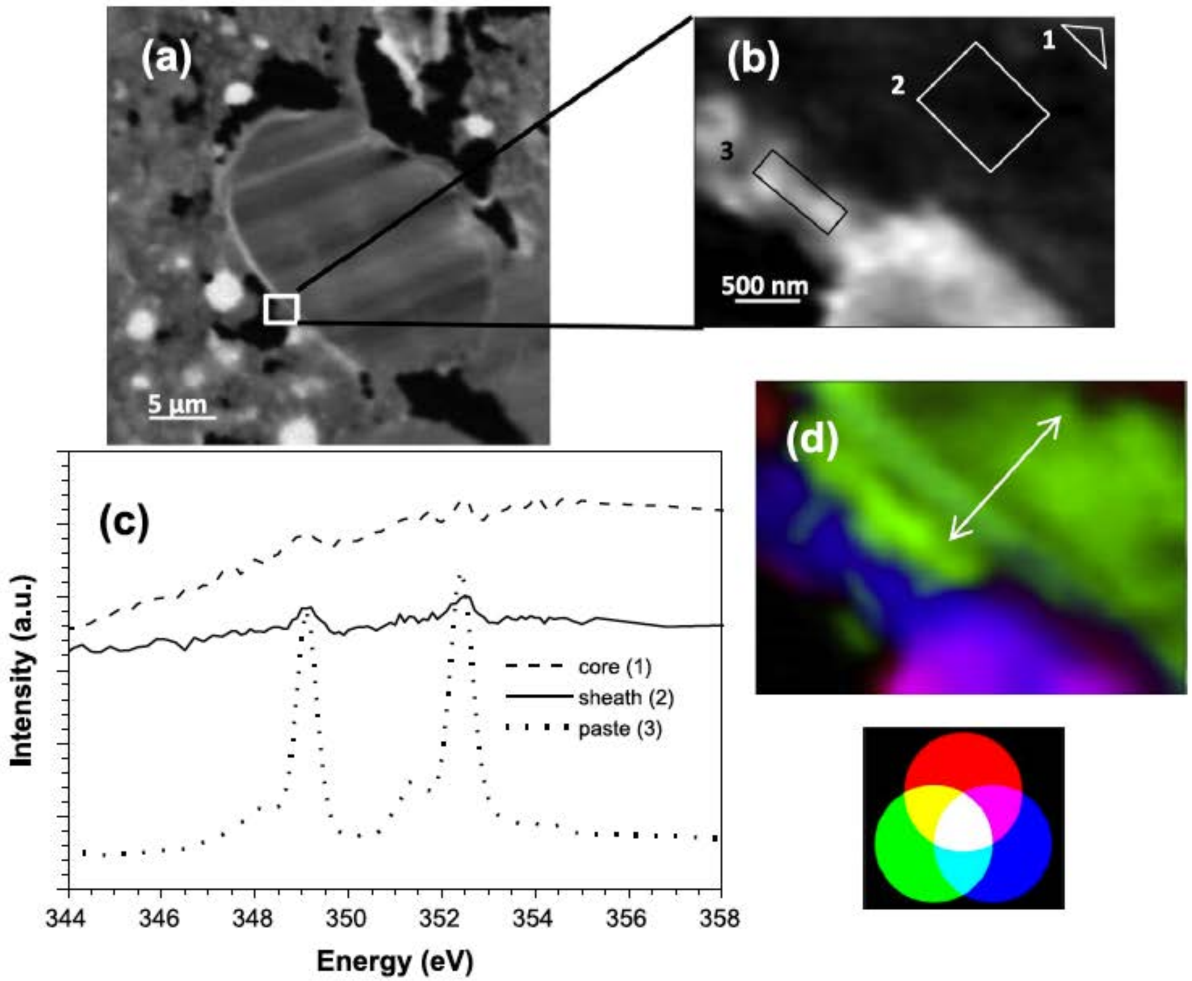

Fig. 7. (a) An OD image showing the area where a Ca image stack was obtained; (b) the OD image extracted from the image stack showing the three areas where the NEXAFS spectra were extracted (c) the NEXAFS spectra extracted for the three areas representing the PP core (1), the EAA sheath (2), and the clear and strong spectra of the HCP area (3); and (d) the RGB composite map showing the PP core in red, the EAA sheath in green, and the HCP in blue. (For interpretation of the references to color in this figure legend, the reader is referred to the web version of this article.)

What about Afm and Aft?

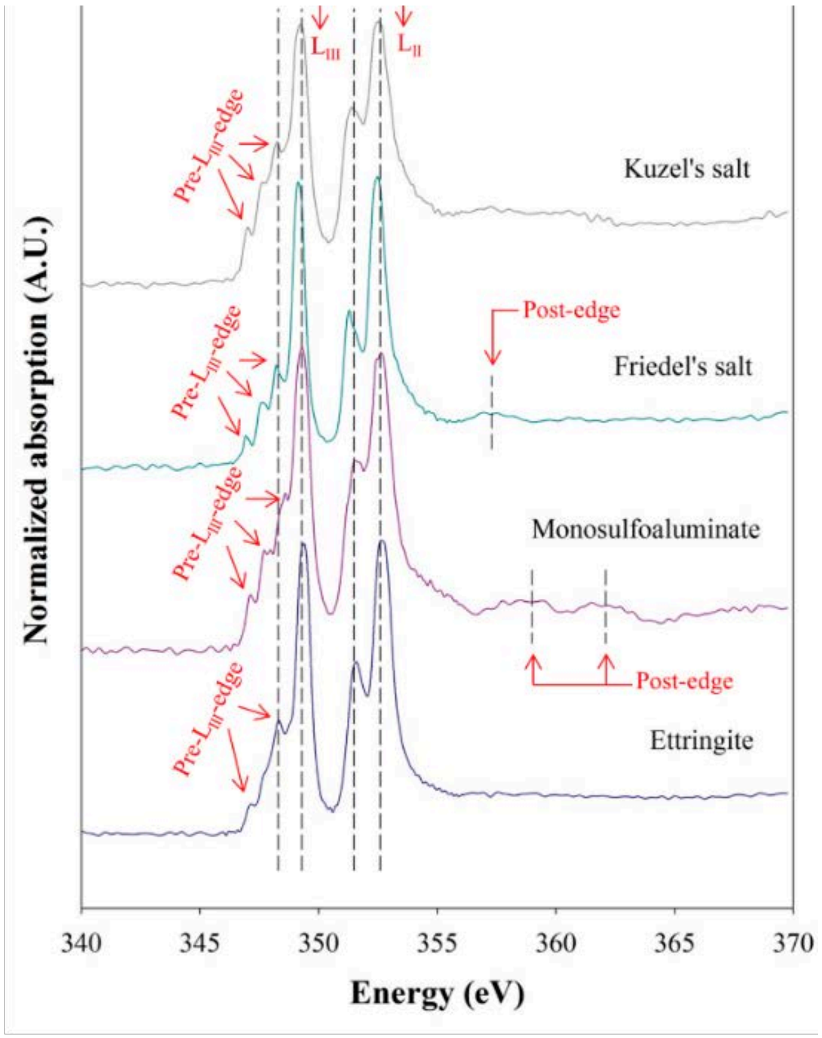

Mineral Name		AFm Phase			AFt Phase
		Friedel's Salt	**Kuzel's Salt**	**MonosulfoalumInate**	**Ettringite**
Intensity ratio	a_2/a_1	2.77	1.36	1.87	2.56
	b_2/b_1	1.86	1.23	1.93	1.70
Peak position (eV)	Pre-L_{III}-edge	346.9 347.6 348.2	347.0 347.6 348.3	347.1 347.8 348.6	347.2 348.3
	L_{III}-edge	349.2	349.2	349.3	349.4
	Pre-L_{II}-edge	351.3	351.37	351.6	351.6
	L_{II}-edges	352.5	352.57	352.6	352.6
	Post-edge	357.3	N.D.	359.0362.1	N.D.
Atomic distribution in the first shell of Ca			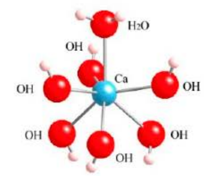		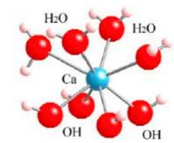

N.D.: Not Detected.

STXM images of NaCl-reacted monosulfoaluminate samples

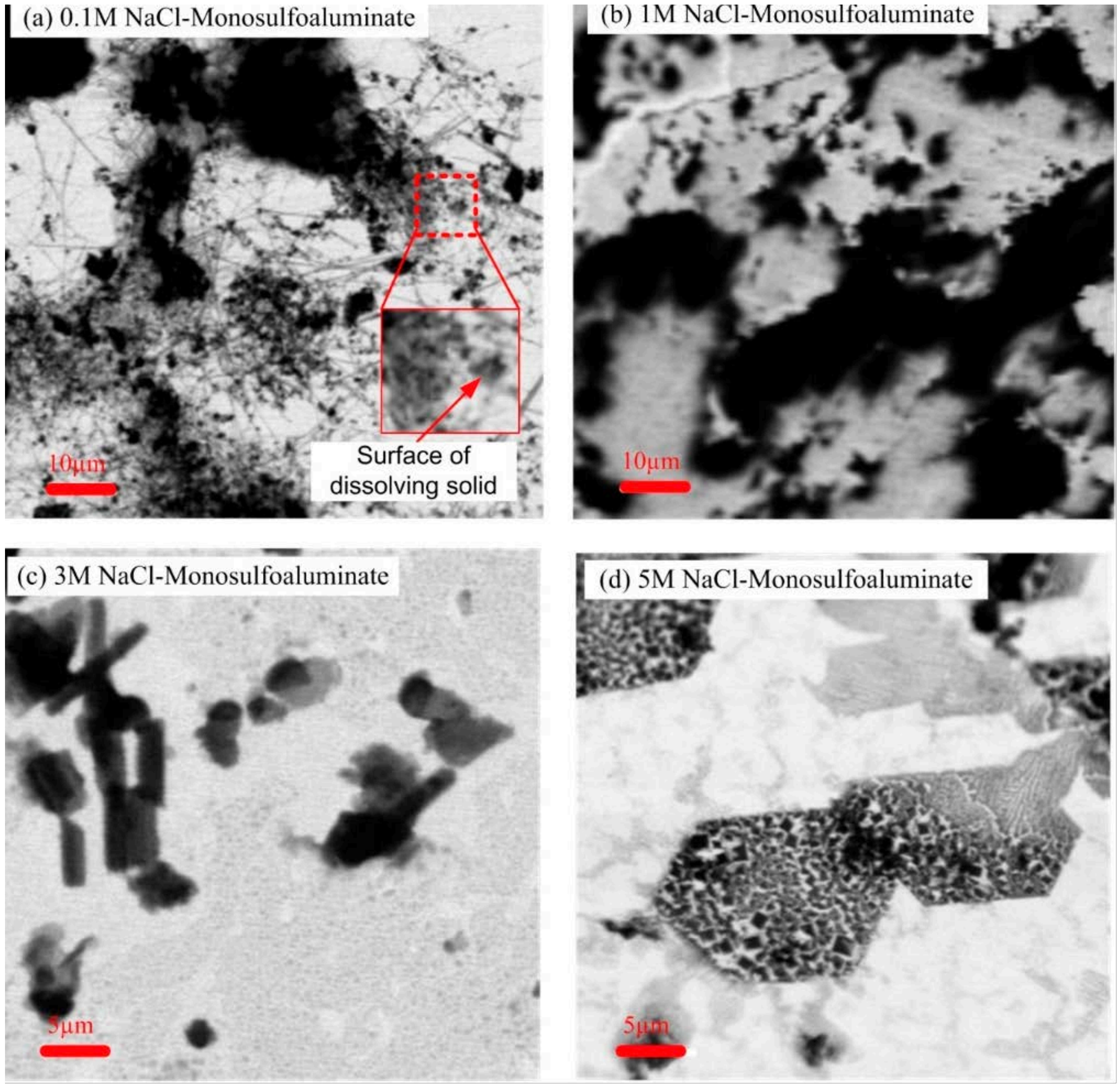

Effect of chemical admixtures

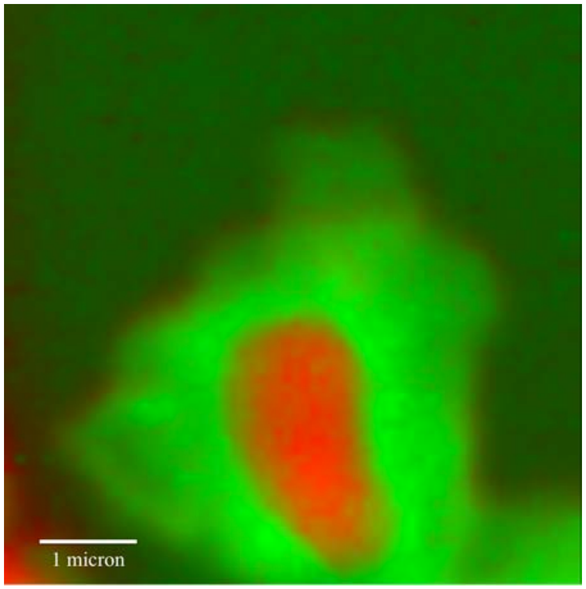

C_3S (reference)

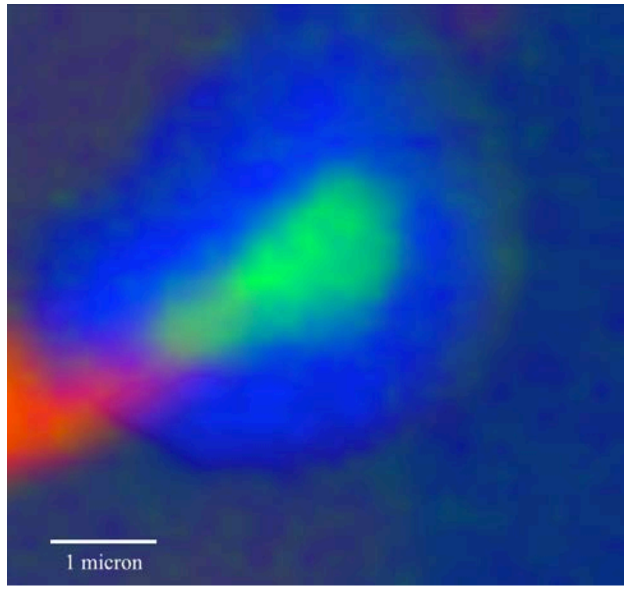

C_3S + PCE-Sil

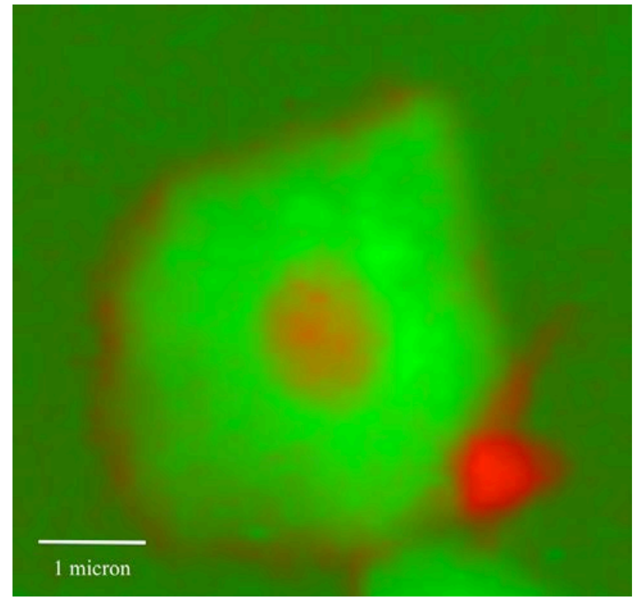

C_3S + PCE

Towards very high spatial resolution nanotomography

Soft X-ray nanotomography work done at BESSY, Berlin

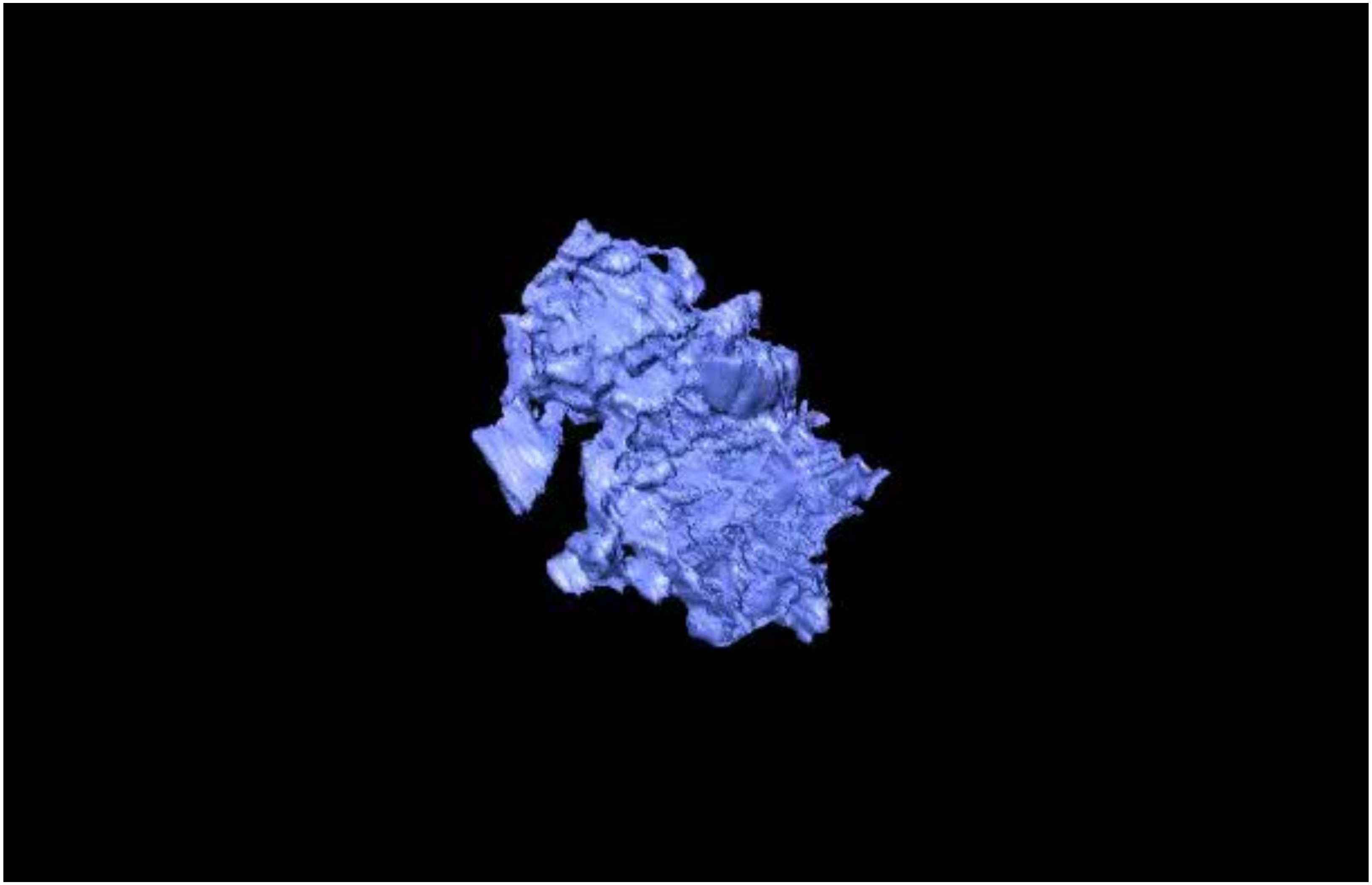

Jackson et al. JACers, 2013.

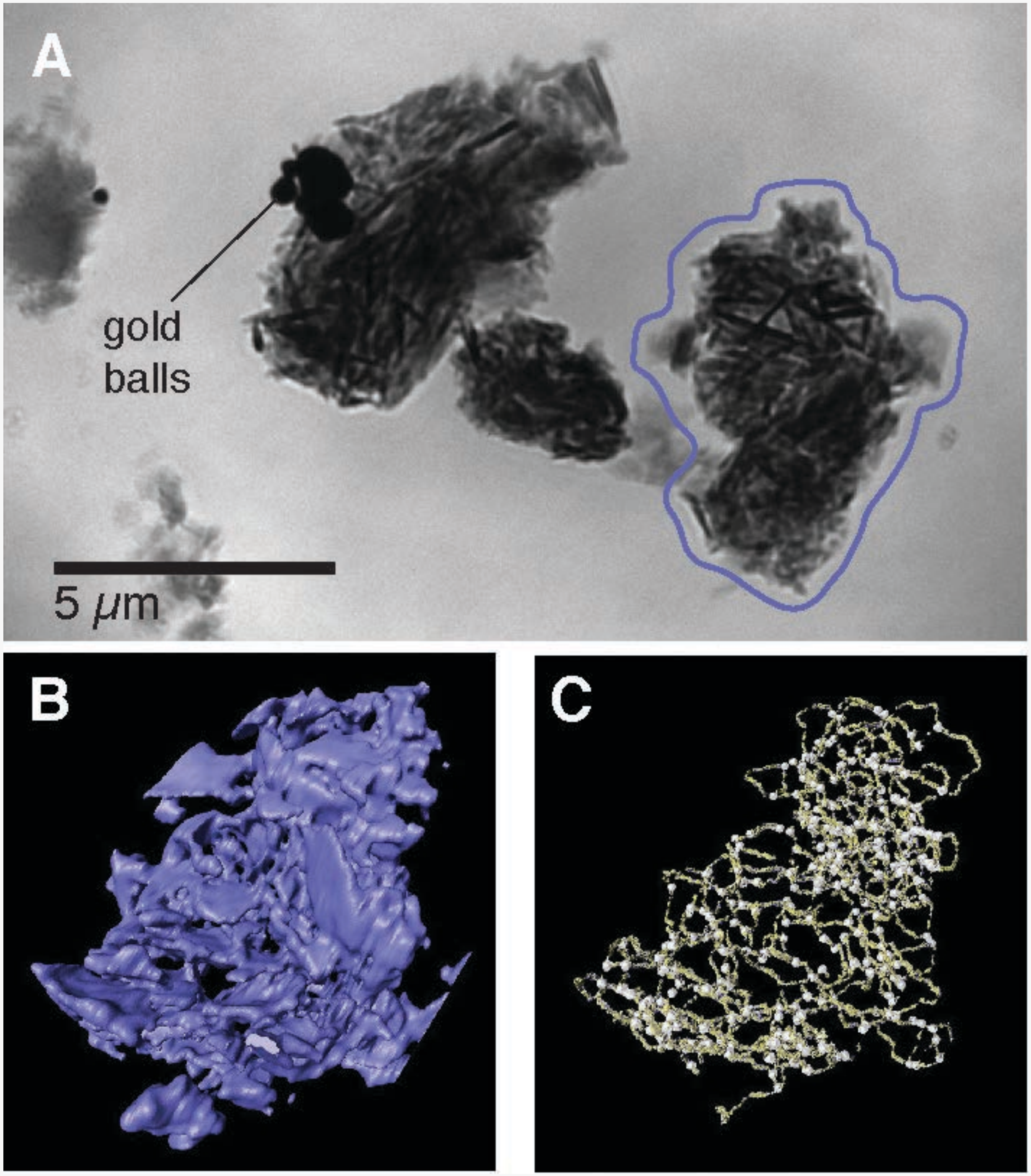

Soft X-Ray Nanotomography

Work done at BESSY, Berlin

Jackson et al. Journal of American Ceramics Society, AUG 2013.

Bridging the gap from nano to micro length scales

Application of the 2D Fourier slice theorem:

Consider one projection $A(x,y)$;

1. Take the 2D Fourier transform of $-\ln(A(x,y))$ to obtain the complex function $A_c(q_x, q_y)$;
2. The spectral density $P(q_x, q_y)$, of $-\ln(A(x,y))$ is

$$P(q_x, q_y) = A_c(q_x, q_y) \bullet A_c^*(q_x, q_y)$$

The spectral density is a good approximation of the small angle scattering pattern, $I(q_x, q_y, q_z=0)$

Portland cement paste

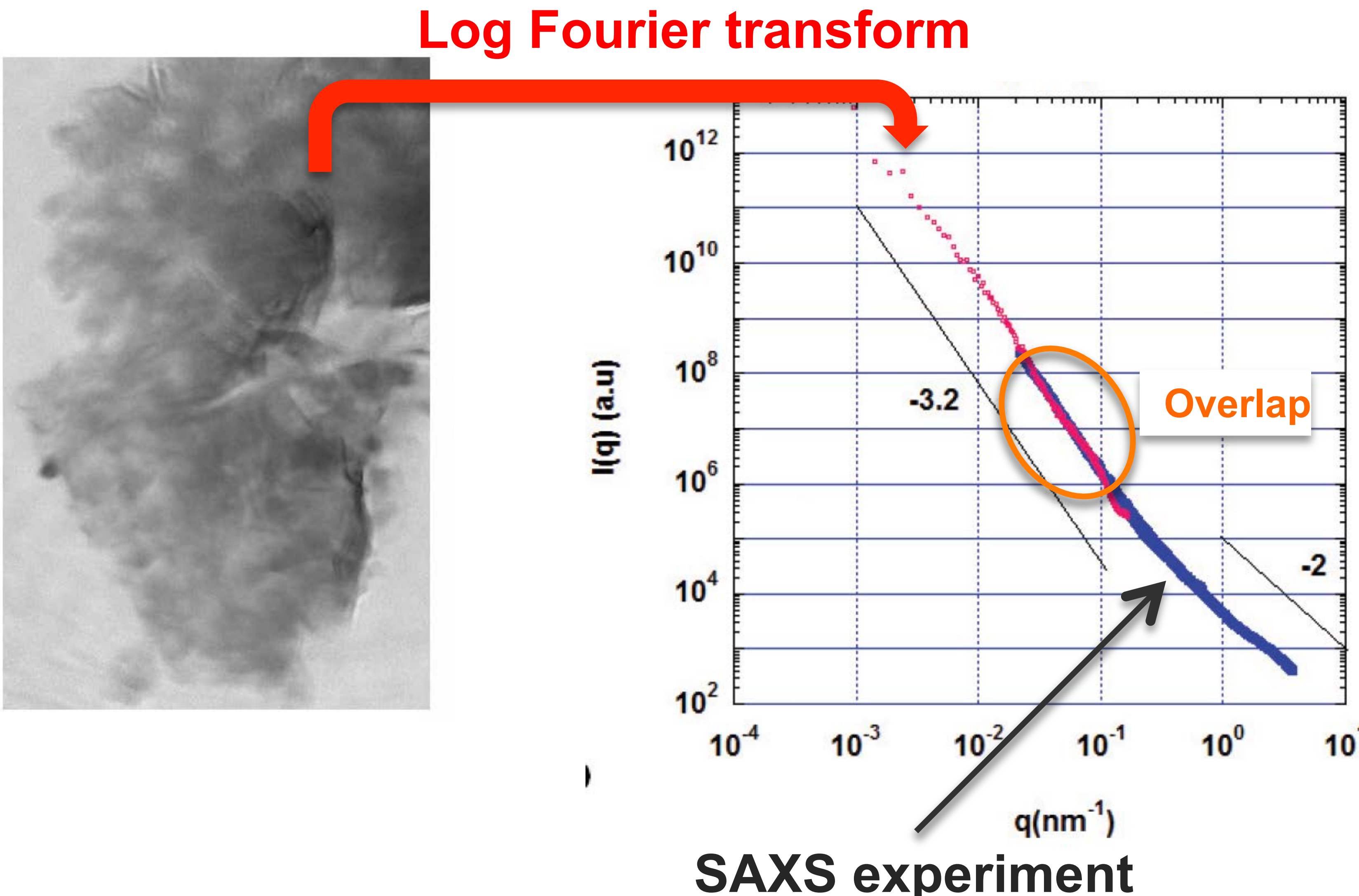

Brisard et al., Am. Min., 2012

nature

Vol 435|30 June 2005|doi:10.1038/nature03719

LETTERS

Soft X-ray microscopy at a spatial resolution better than 15 nm

Weilun Chao[1,2], Bruce D. Harteneck[1], J. Alexander Liddle[1], Erik H. Anderson[1] & David T. Attwood[1,2]

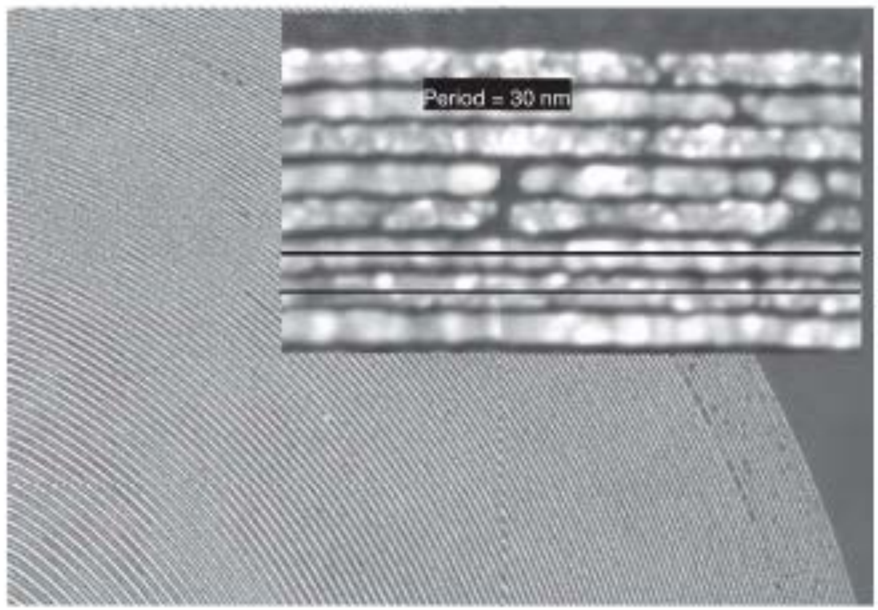

Figure 3 | Scanning electron micrograph of a zone plate with 15 nm outermost zone. Shown in the inset is a more detailed view of the outermost zones. The zonal period, as indicated by the two black lines, is measured to be 30 nm. The zone placement accuracy is measured to be 1.7 nm.

Ptychography

A major breakthrough in high resolution x-ray imaging

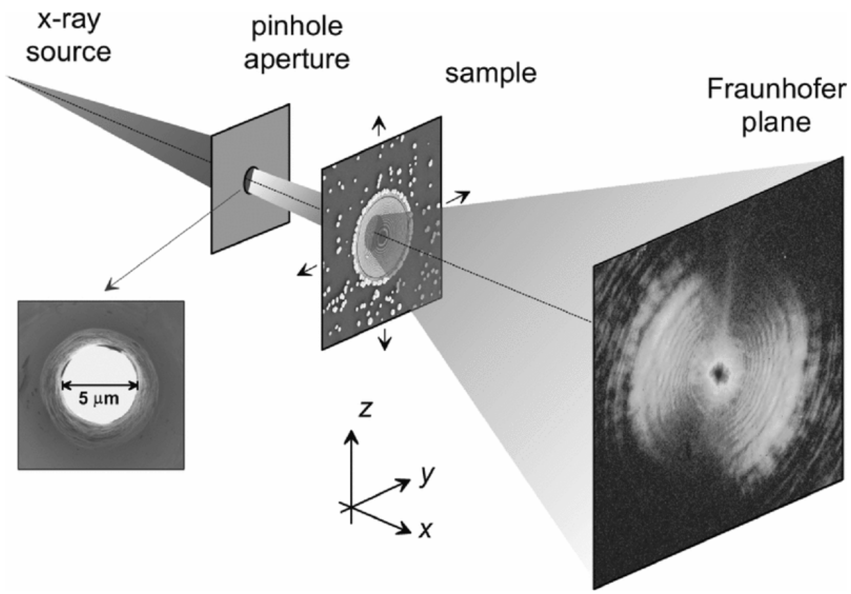

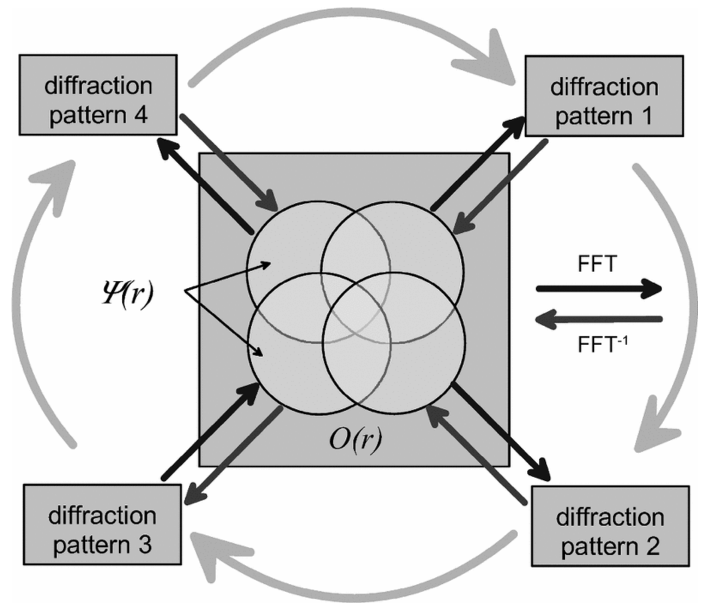

J. M. Rodenburg et al., PRL, 2007

Advantage of redundant data

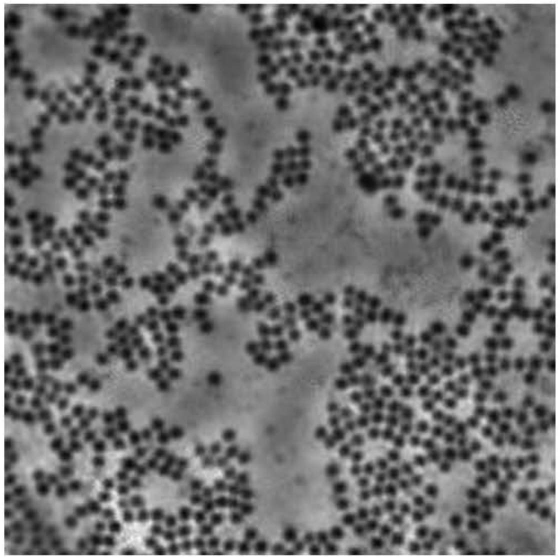

Object is split into frames with known centers
Each frame is illuminated separately
Neighbors overlap

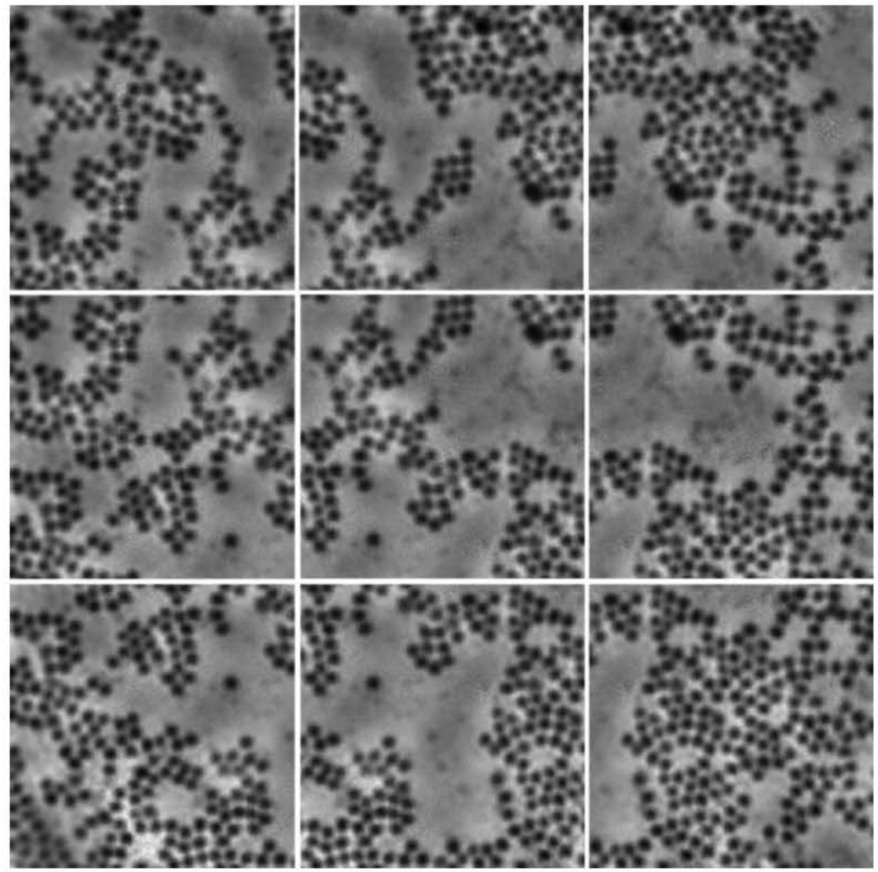

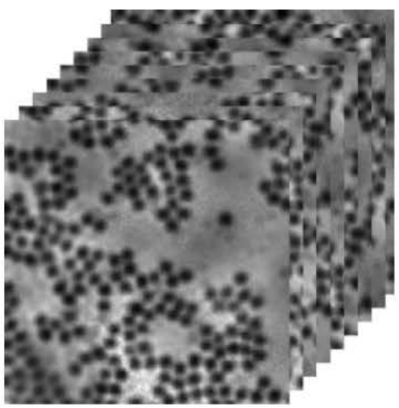

From David Shapiro

Nanosurveyor 1.0 – ALS Beamline 5.3.2.1

- 7 s / μm^2 measurement time
- 5-10 nm resolution
- 2 nm RMS stability
- Open geometry, EASY TO USE
- 25-250 nm zone plate
- Up to 25 mm focal length, 100 μm depth of field
- No cryo

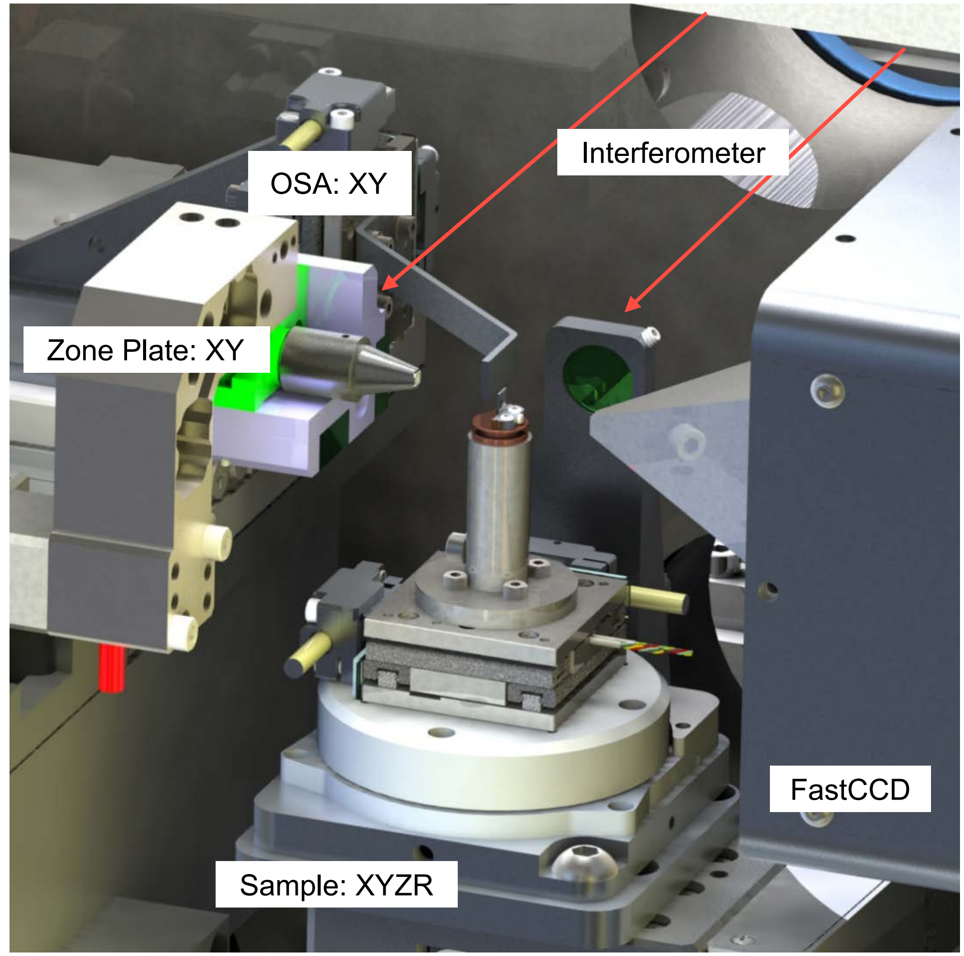

Ptychography with soft x-rays (work done at the Advanced Light Source)

Log Fourier transform

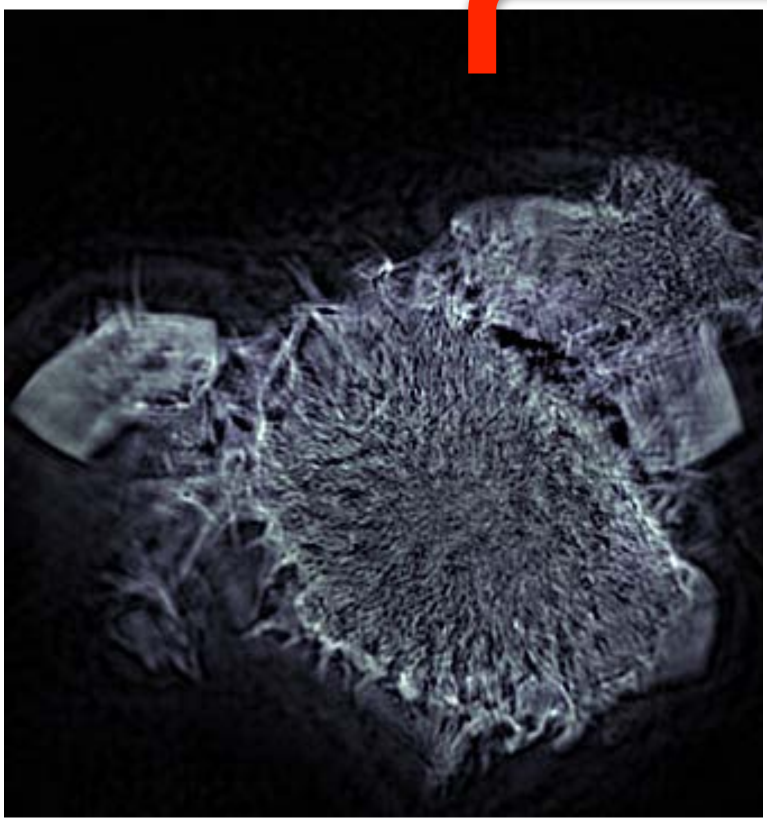

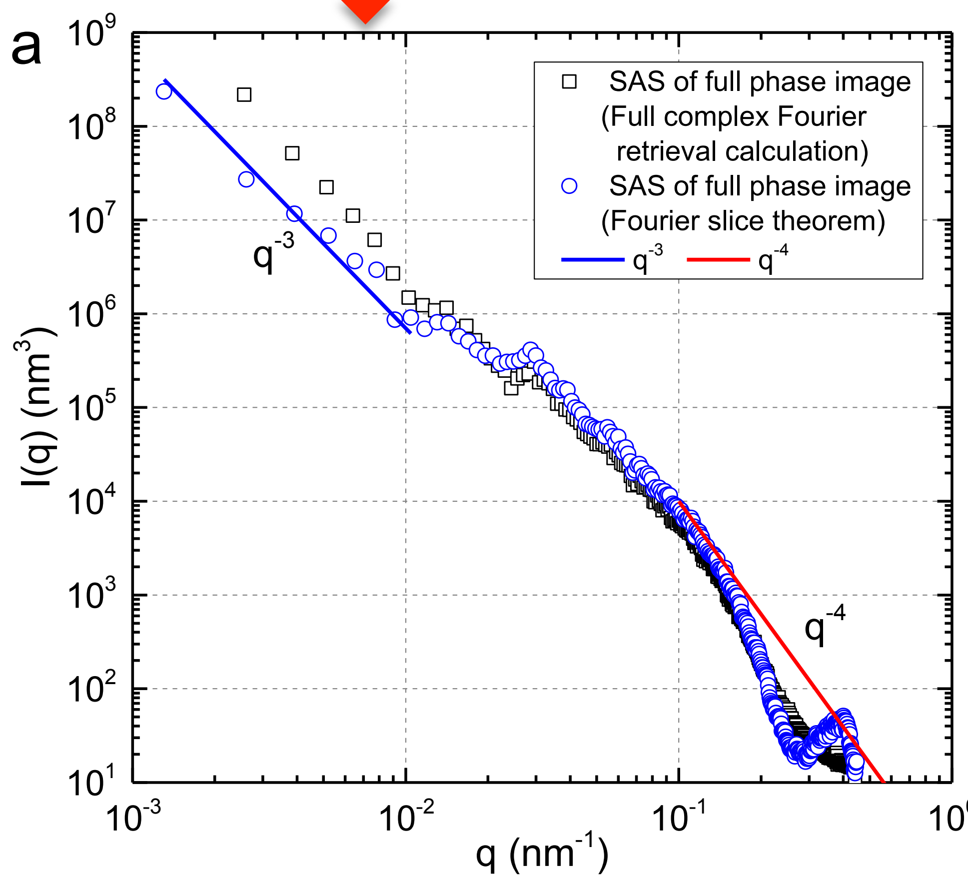

Bae et al., JACers, 2015

With such high spatial resolution it is possible to probe the inner product

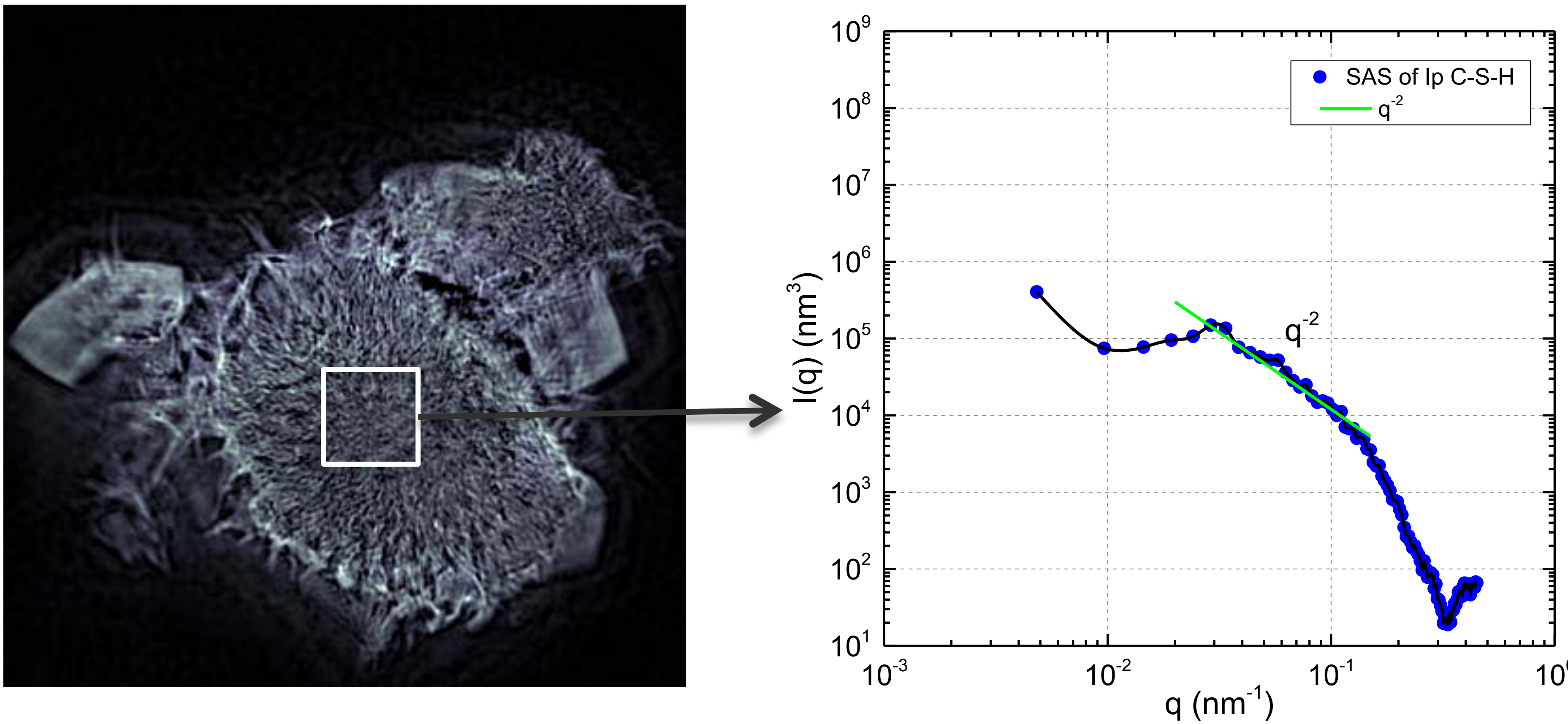

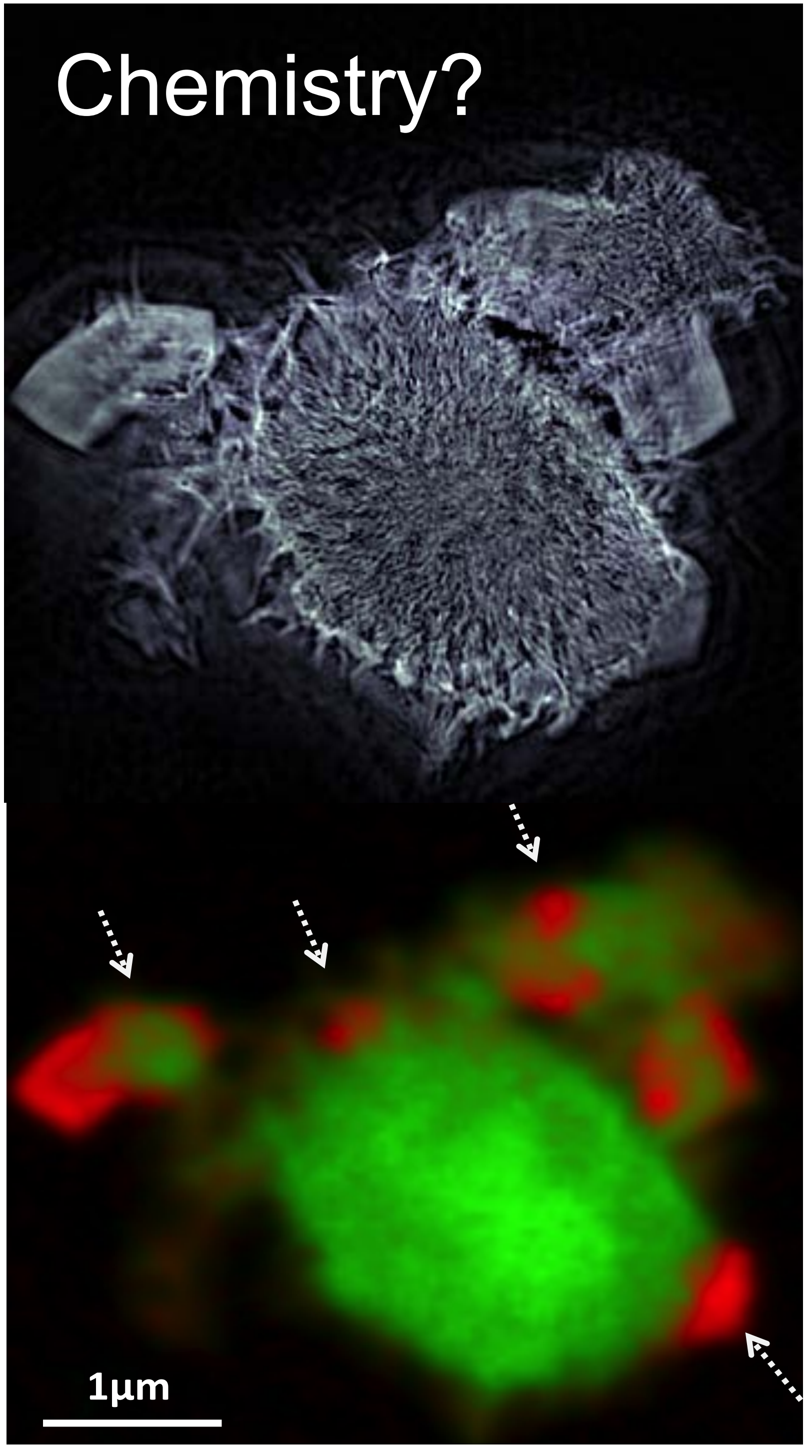

XANES with
Soft X-Ray Transmission Microscopy

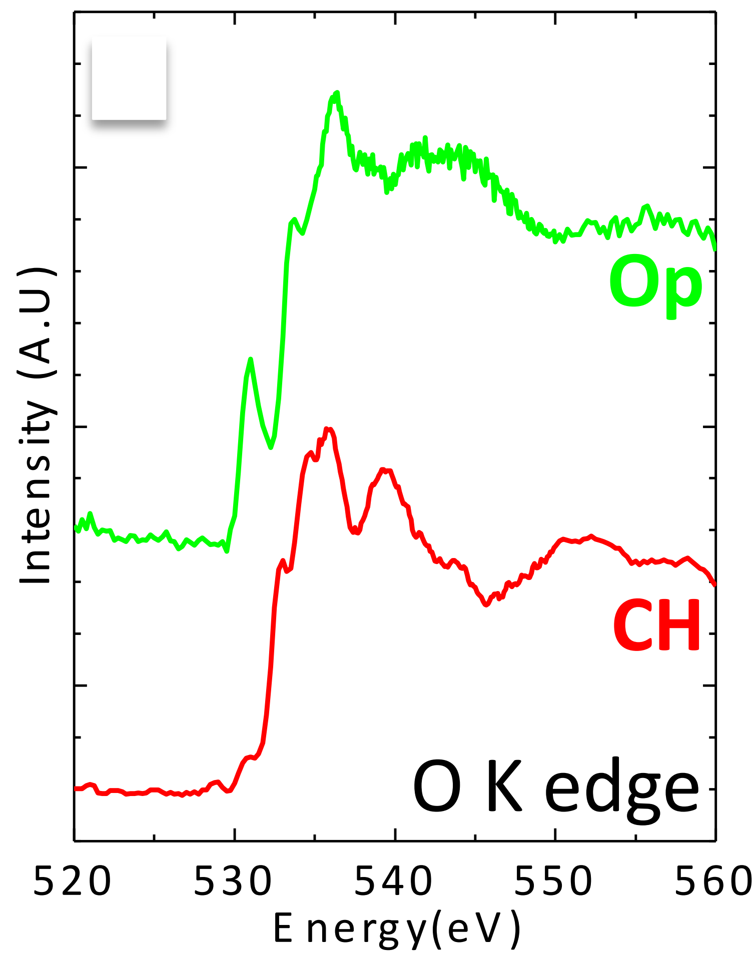

Final Question:

Is it possible to obtain nanoCT with extremely high spatial resolution?

Collaborators

- Pierre Levitz
- G.I. Barenblatt
- S. Brisard
- K. Kurtis
- G. Geng
- C. Bae
- D. Shapiro
- C. Ostertag

Rossella Pignatelli
Claudia Comi
M. D. Jackson
S. Yoon
Daniel Hernandez Cruz
David A. Kilcoyne
P. Guttmann